Role of ATF4 in Dietary Sulfur Amino Acid Restriction

By

Nicholas Margolies

A thesis submitted to the

Graduate School – New Brunswick

Rutgers, The State University of New Jersey

in partial fulfillment of the requirements

for the degree of

Master of Science

Graduate Program in Endocrinology and Animal Biosciences

written under the direction of

Dr. Tracy G. Anthony

and approved by

_____

_____

_____

New Brunswick, New Jersey

October 2018

ABSTRACT OF THE THESIS

Role of ATF4 in Dietary Sulfur Amino Acid Restriction

by NICHOLAS MARGOLIES

Thesis Director:

Dr. Tracy G. Anthony

Dietary sulfur amino acid restriction (SAAR) increases food intake and energy expenditure and improves body composition. Dietary SAAR activates the integrated stress response (ISR), which orchestrates transcriptional changes through activating transcription factor 4 (ATF4). Fibroblast growth factor 21 (FGF21) is a hepatokine and ATF4 target which affects food and fluid intake, energy expenditure, and body composition. To determine whether ATF4 is needed to increase food and fluid intake and energy expenditure, improve body composition, and alter hepatic gene expression during SAAR, male and female wild type (WT) and *Atf4*$^{-/-}$ (KO) mice were maintained on a high fat (60% fat by Kcal) control (0.86% Met, 0% Cys) or high fat SAAR (0.12% Met, 0% Cys) diet for 5 weeks. SAAR increased hepatic *Fgf21* and water intake independently of ATF4 in males and females. In males, SAAR increased food intake and energy expenditure independently of ATF4, while females showed no response. SAAR improved body composition in WT males but not females and did not prevent increased adiposity in male KO mice. ATF4 is required for protection from adiposity but not for increased food and water intake, energy expenditure, or hepatic *Fgf21* expression during SAAR. FGF21 does not work exclusively through an ATF4-FGF21 axis and may be driving ATF4-independent responses to SAAR.

Acknowledgements

Dr Anthony, thank you for your excellent mentorship (and high standards!). My time in your lab has helped me improve both professionally and personally, and I am grateful for that.

Thank you also to Dr Bello and Dr Belden, for your feedback in reviewing the data. Your comments provided valuable direction and are much appreciated.

I would also like to acknowledge the lab. Emily, you make the lab a home. You are so much more than the title ‘lab manager’ could ever describe, and I hope you know how amazing you are! Ashley, thank you for introducing me to this topic. Inna, you inspire me constantly with the quality of your work. Dylan and William, you always brighten up the office. You are all some of the strongest, kindest people I have ever met. It was an honor to work with you, and I’m proud to call you friends.

This work would not be complete without the efforts of undergrads: Eugenia Saeigh, who processed data from earlier cohorts, and Megan Hupp, who did some of the qPCR.

Thank you to the many teachers and professors I have had over the years, for your love of what you do. You have been a great positive influence in my life.

Thank you to Dr Ralston and Bill for taking my old buddy JJ into your family, giving him a wonderful home for the rest of his life, and for your generosity in so many other ways. I could never have dreamed of a better miracle.

Thank you to my dad for my undergraduate education, letting me start my life without debt, and for being my safety net no matter what emergency may arise. Thank you to my

mom for raising me to be idealistic, enthusiastic and hopeful. Thank you to my grandparents for your guidance and wisdom over the years.

Thank you to my friends for helping me help myself, and for being my light at the end of the tunnel. Together we can do some good! Thanks for being with me on this journey. I couldn’t do it alone.

Table of Contents

List of abbreviations

SAAR: sulfur amino acid restriction

ISR: integrated stress response

ATF4: activating transcription factor 4

FGF21: fibroblast growth factor 21

CR: caloric restriction

PR: protein restriction

MR: methionine restriction

GCN2: general control nonderepressible 2

eIF2: eukaryotic initiation factor 2

CREB2: cyclic AMP response element (CRE) binding protein 2

C/EBP: CCAT enhancer binding proteins

CARE: C/EBP-ATF4 response elements

AARE: amino acid response element

uORFs: upstream open reading frames

UMAI: uORF-mediated ATF4 indicator

List of Figures and Tables

CHAPTER 1: REVIEW OF LITERATURE

Introduction

Caloric restriction (CR) is an effective, but severe strategy to combat obesity and associated health risks. Protein restriction (PR) recapitulates some beneficial effects of caloric restriction, without reducing calories [1]. Notably, while CR reduces energy expenditure [1, 2], ad lib feeding of PR in rodents increases both intake and energy expenditure [3]. This reduces fat mass without wasting muscle. The protein leverage hypothesis, which has also been extended to individual amino acids, explains these effects as a series of compensatory events [4]. Hyperphagy is seen as an effort to achieve sufficient protein intake while consuming a protein 'diluted' diet [5]. To offset increased energy consumption, metabolism must then become less efficient. Deprivation of a single amino acid, despite normal protein levels, is sufficient to trigger some effects of PR [6]. Moreover, both dietary methionine restriction (MR) and dietary leucine restriction (LR) increase energy expenditure and weight loss without reducing food intake[7, 8], but dietary MR reduces hepatic lipogenic gene expression while dietary LR does not. The mechanisms which explain metabolic responses to loss of protein versus individual amino acids remain to be fully understood.

Amino acid stress is sensed by general control nonderepressible 2 (GCN2), one in a family of 4 kinases reactive to specific environmental stressors. These kinases converge at the point of eukaryotic initiation factor 2 (eIF2), phosphorylating it and triggering an adaptive response called the integrated stress response (ISR). This response includes increased translation of activating transcription factor 4 (ATF4). As a transcription factor,

ATF4 increases both its own transcription and that of targets such as fibroblast growth factor 21 (FGF21), which alters food intake, energy expenditure, body composition and hepatic gene expression. Despite the direct relationship between GCN2 activity and ATF4 translation, GCN2 independent responses to dietary MR are reported [9, 10], and loss of *Gcn2* versus *Atf4* produces different effects in liver during asparagine depletion [11]. In consideration of these findings, it is important to investigate the role of ATF4 during dietary amino acid insufficiency such as sulfur amino acid restriction (SAAR).

Sulfur Amino Acid Restriction is a unique amino acid stress

For over 25 years dietary MR has been studied using diets that are zero cysteine plus methionine-reduced 80%-85% by dry weight [12]. This level of dietary MR causes growth stunting in growing rats [13] but in mature rodents promotes leanness and longevity. In fact, MR diets were first studied in regard to lifespan extension [12, 14], then subsequently attracted attention for their ability to decrease fat mass without muscle wasting despite increased food intake [9, 15]. Importantly, repletion of cysteine abolishes all metabolic effects linked to increased insulin sensitivity and energy expenditure by MR [6]. A zero methionine and very low cysteine (.0 g/100g diet) also induces similar effects [16]. Thus, because the level of cysteine is important to the overall metabolic phenotype, it is more appropriate to describe these diets as sulfur amino acid restriction (SAAR) versus MR.

The importance of removing cysteine from the diet completely during SAAR [6] points to nuances in one-carbon metabolism that may mediate certain benefits. SAAR through a

cysteine-devoid methionine-sufficient diet alters serum levels of other downstream products of methionine, such as cystathionine, taurine, and homocysteine [17]. It is interesting that SAAR is able to prevent the progression of hepatic steatosis [18] and that dysregulated sulfur amino acid metabolism occurs during the progression of nonalcoholic fatty liver disease (NAFLD) to steatosis[19]. It is possible that, in addition to triggering metabolic responses similar to protein and caloric restriction, SAAR may have unique effects by ameliorating dysregulated sulfur amino acid metabolism.

SAAR may also act uniquely through histone methylation and ornithine mediated signaling [20]. In MC57 breast cancer cells and PC3 prostate cancer cells, methionine restriction altered expression of many of the genes changed by methionine deprivation, albeit more modestly [20]. Methionine deprivation created the most dramatic unique gene signature of all the amino acids and reduced intracellular S-adenosyl-Methionine (SAM), S-adenosyl-Homocysteine (SAH), and 5’ Methylthioadenosine (MTA) [20]. SAM is a universal donor for the methylation reaction that modifies DNA, histones, and other proteins. Accordingly, methionine deprivation reduced the histone methylations H3K4me2, H3K4me3, H3K9me2, and H3K9me3 [20].

SAAR has a broad range of positive health impacts, such as improving biomarkers of oxidative stress [21] and reducing serum glucose, insulin [9] and IGF1 [9, 22]. Cataract development is delayed [23]. Arrhythmogenic, hypertrophic, and cardiomyopathy signaling pathways in the heart are downregulated [23], and SAAR mice have an attenuated cardiac response to beta adrenergic stimulation [23]. Despite smaller skeletal

frames corresponding with their smaller body sizes, bones of SAAR mice have improved intrinsic strength [24]. SAAR is able to confer the same level of protection from acetaminophen induced liver damage as 60% caloric restriction [22], and prevents the progression of hepatic steatosis in ob/ob mice [18]. SAAR is also involved in the benefits of a ketogenic diet, as methionine supplementation reverses weight loss, reduces the increase in energy expenditure, and normalizes changes in gene expression [25] which result from a ketogenic diet.

Most notably in the context of obesity prevention, SAAR increases energy expenditure [26] as well as heat increment of feeding. SAAR also reduces fat deposition both overall [26] and in inguinal, epididymal, and reptroperitoneal fat pads specifically [9] and provokes browning of white adipose tissue [26]. In adipose there is also increased expression of fatty acid oxidation genes [18], decreased expression of lipogenic genes such as SCD1 [18], and a more complete shift to fatty acid oxidation on a whole body level [26]. Triglyceride content in serum [9] and liver [18] are also decreased.

Dietary restriction of leucine (LR) to a similar level as SAAR creates a similar whole-body phenotype. Although leucine deprivation suppresses food intake, LR has been shown to create a hyperphagic response resembling SAAR [7] or at least to have no effect on intake [8]. Both LR and SAAR increase energy expenditure and reduce body weight. However, SAAR has a greater effect on body composition and hepatic gene expression [7, 8], so it is likely that specific amino acid sensing pathways exist in addition to a more general pathway for all amino acid stress.

The Integrated Stress Response

The ISR integrates signals for multiple environmental stressors into a unified response. It involves a family of kinases which act as initial stress sensors, a common phosphorylation target upon which these kinases converge, and a change in mRNA translation which directly and indirectly alters the activity of the cell. The stress sensors of the ISR are 4 different eIF2-kinases: PERK, which responds to ER stress; HRI, which responds to heme deprivation in erythroid cells; PKR, which responds to viral infection; and GCN2, which responds to amino acid stress [27]. Phosphorylation of eIF2 by GCN2 during amino acid stress leads to increased translation of activating transcription factor 4 (ATF4), which then orchestrates an adaptive transcriptional response.

This cascade, in which GCN2 is the sensor, phosphorylated eIF2 is the "core," and ATF4 is the effector, is the canonical amino-acid-stress arm of the ISR [27] Because it is phospho-eIF2's effects on translation initiation which truly enable the adaptive response, and this translation control appears to occur sometimes without increased phospho-eIF2 [28], I believe it is more appropriate to designate translational control itself as the core. Further, because the targets of ATF4 are important in creating a whole-body phenotype characteristic of amino acid stress, I believe it is important to include them in the scheme of the ISR as "mediators". Although the amino acid arm of the ISR was initially delineated as a GCN2-eIF2-ATF4 pathway, recent literature brings more complexities to our understanding, which are discussed in later sections and shown visually in Illustration 1.

GCN2: an ISR "sensor"

In agreement with the sensor-core-effector understanding of the ISR, genetic deletion, or knockout (KO) of *Gcn2* impairs adaptation to amino acid deprivation. Whole body genetic deletion of *Gcn2* dramatically impairs the ability of mice to adapt to amino acid deprivation. *Gcn2* KO mice deprived of leucine for 6 days experienced significant mortality [29]. Those mice which did survive were able to defend normal levels of protein synthesis in their livers, but at the expense of their skeletal muscle, a consequence which wild type mice were able to avoid [29]. Furthermore, *Gcn2* KO mice on a leucine free diet had increased liver triglycerides, and steatosis as detected by Oil Red O and Hematoxylin and Eosin staining [30]. They also had increased serum free fatty acids, rather than decreased as seen with wild type mice [30].

GCN2 is involved not only in adapting cellular activities to survive nutritional stress, but in behavioral aversion to those diets which will not support life. *Gcn2* KO mice fail to immediately reject diets lacking either leucine [31] or threonine [32], although hours and days later they display a reactive anorexia similar to wild type mice [29, 33]. Consuming insufficient diets can also be catastrophic to the next generation. Offspring of *Gcn2* KO mice whose mothers were fed a leucine- tryptophan- or glycine-deficient diet during gestation experienced significantly more mortality pre- and post-natally [34].

GCN2 is also necessary during amino acid deficiency. Mice lacking branched chain alpha keto acid dehydrogenase kinase (*Bdk* KO) are deficient in leucine, isoleucine, and valine [35, 36]. As shown by She et al[37] *Bdk* KO mice display neurological abnormalities as well as activation of the ISR in brain. *Bdk* KO mice are muscle growth stunted, yet still manage survive into adulthood [37]. Successful ISR activation may be what allows them to reach maturity with only neurological abnormalities, rather than dying quickly. Mice which are homozygous null for both *Gcn2* and *Bdk* cannot induce the ISR in response to branched chain amino acid deficiency, and do not survive past postnatal day 15 due to a block in myelin formation in the central nervous system resulting from the premature death of developing oligodendrocytes [37].

GCN2 activation and eIF2 phosphorylation, triggered by ribosome stalling, was also found associated with a mutation which rescued mice in a model of neurodegeneration [38]. Ishimura et al identified induction of ISR genes in this model and in models of amyotrophic lateral sclerosis [39] and Alzheimer's [40], suggesting the broad impact of the ISR in maintaining brain health.

Translational Control: the ISR "core"

Upon registering reduced amino acid availability through GCN2 activation and phosphorylation of its target, eIF2, the ISR involves changes in mRNA translation which alter cell activity directly and indirectly [27]. The selective translation of some transcripts during reduced global translation, such as occurs during the ISR, is called translational

control (TC). There is a complex mechanism through which phosphorylated eIF2 (phospho-eIF2) represses the initiation phase of protein synthesis. However, it appears translational control may also occur without elevated phospho-eIF2 [28]. With this in mind, although phospho-eIF2 has previously been considered the "core" of the ISR [27], I will assign this designation to translational control instead (Illustration 1). It is TC, regardless of how it is achieved, upon which adaptive cellular responses hinge. Repression of global translation conserves resources during times of amino acid scarcity, and gene-specific translation during stress allows the translation of necessary regulatory factors (such as ATF4) to trigger a homeostatic response appropriate to address it.

In the classical GCN2-activated sense, we have an excellent idea of how translational control is initiated and, eventually, self-inhibited (one of ATF4's main targets, growth arrest DNA damage 34 (GADD34), reduces the phosphorylation of eIF2). GCN2 senses amino acid deprivation through binding of uncharged tRNA to a domain structurally similar to histidinyl tRNA synthetase; this domain is not necessary for GCN2 dimerization, but interacts with the kinase domain and is critical for GCN2 function *in vivo* [41]. Upon binding of uncharged tRNA, GCN2 dimerizes and phosphorylates the alpha subunit of eIF2 on serine residue 51 [42-47].

The events following eIF2 phosphorylation which lead to translational control are well reviewed [48]. eIF2 is one of many eIFs required to assemble a competent ribosome. The effects of its phosphorylation may be best understood in comparison to its role when functioning normally. Formation of a competent ribosome is a multi-step process

involving numerous factors. eIF2 becomes part of a ternary complex including GTP and Met-tRNA. This ternary complex then joins other eIFs – eIF3, eIF1, eIF1A, and eIF5 – in binding the 40S ribosomal subunit. What is formed is not yet a competent ribosome, but only a precursor known as the 43S preinitiation complex (PIC). The 43S PIC must acquire other protein factors, such as the eIF4 complex, to mature into a 48S PIC. Finally, it is this 48S PIC which scans mRNA in the 5' to 3' direction. Normally, eIF2 plays a critical role in the recognition of a start codon by the 48S PIC. At that codon, eIF2-associated GTP is hydrolyzed, and the anticodon loop of the initiator methionyl tRNA base pairs with the initiation codon in the P site of the 40S subunit. Recognition of the start codon is the last hurdle to translation. Thanks in part to the role played by eIF2, 40S and 60S subunits assemble into a competent 80S ribosome ready for translation elongation.

In order for translation to continue, the GDP hydrolyzed during recognition of the start codon must be exchanged for GTP. Under normal conditions, this exchange proceeds without difficulty and is catalyzed by the tetrameric guanine nucleotide exchange factor (GEF) known as eIF2B. The GDP to be exchanged is bound to eIF2. During stress, the phosphorylated serine residue on eIF2's alpha subunit interacts with the regulatory subcomplex of eIF2B, competitively inhibiting its GEF activity. Some GDP-to-GTP exchange does occur, but it takes longer, and this dramatically shifts the profile of which mRNAs are translated.

Translation of most mRNAs is reduced by translational control, because GTP must be available for hydrolysis the moment would-be ribosomes encounter a start codon. When eIF2 is phosphorylated, or under any other condition which reduces guanine nucleotide exchange, the 48S PIC scans past the start codon; the initiator methionyl tRNA never base pairs; it misses its chance. In the case of preferentially-translated mRNAs, such as *Atf4*, this missed start codon is not the end but the beginning. *Atf4*'s 5' leader structure contains additional start codons. There are two open reading frames upstream of the *Atf4* coding sequence, known as uORFs (upstream Open Reading Frame). The first, uORF1, is relatively benign regarding *Atf4* translation, as a short (3 residue), positive cis acting element. uORF1 merely encourages re-initiation at uORF2, but uORF2 – at a much longer 59 residues – overlaps out of frame with the primary *Atf4* coding region. Translation of uORF2 means the start codon of *Atf4* is never seen by the 48S PIC, and ATF4 is never made. During stressed conditions, translation initiation is delayed, scanning ribosomes bypass uORF2's start codon, and *Atf4* is translated instead.

ATF4: the ISR "effector"

ATF4 is a member of the ATF family of DNA binding proteins, which has a basic leucine zipper region. It is also known as cyclic AMP response element (CRE) binding protein 2 (CREB2), and ATF and CREB proteins were identified separately but found to be the same. ATF4 forms dimers with other basic leucine zipper (bZIP) transcription factors, such as CCAAT enhancer binding proteins (C/EBP). ATF4 functions as a

transcription factor, which increases expression of multiple genes to maintain homeostasis and avoid apoptosis during stress. The cis sequence elements bound by ATF4 are called C/EBP-ATF4 response elements, or CAREs. However, due to ATF4's role in amino acid stress, the CARE response element is also known as the amino acid response element (AARE).

Classic CARE-containing genes encode amino acid transporters and genes involved in amino acid synthesis, which directly impact homeostasis during amino acid stress. Not all genes that contain CARE/AARE regulate protein homeostasis, however. ATF4 also regulates genes involved in hepatic cholesterol metabolism, and ER stress in mice [11]. Another CARE/AARE gene is FGF21, a nutritionally regulated hepatokine, which itself can initiate adaptive behavioral and metabolic outcomes to low protein diet and amino acid stress [49-51].

Without ATF4, other stress response pathways are unable to resolve the demands placed on the cell, negatively affecting survival. For example, despite a massive change in gene expression in mice lacking *Atf4* (1,155 genes vs 195 in livers of asparagine depleted *Atf4* KO vs WT mice), adaptation to the amino acid depletion agent asparaginase is not possible and apoptosis results [52]. Staining of asparagine depleted wild type livers for fragmented DNA showed less than 20 positively staining cells per section, compared to none in the control, indicating good survival. In contrast, staining of asparagine depleted *Atf4* KO livers showed massive DNA fragmentation, with over 250 positively staining cells per section as compared to about 60 in the control, indicating significantly increased

cell death [52]. This suggests that ATF4's activities as a transcription factor are important in helping the liver adapt to stress.

To monitor the ISR *in vivo*, Iwawaki et al created a mouse model transduced with a construct containing *Atf4* upstream open reading frames (uORFs) and a luciferase encoding region, called uORF-mediated ATF4 indicator (UMAI) [53]. In this model, translation of luciferase is driven by initiation at the same initiation codon as full length ATF4. High luminescence indicates translational upregulation of ATF4 during the ISR. Because ATF4 is also regulated at the transcriptional level and through ubiquitin/proteasome degradation, the uORF-mediated ATF4 indicator (UMAI) construct is an ideal way to assess ISR-specific translational control of ATF4.

With this model, Iwawaki et al showed whole body luminescence in male and female 12 week old mice in response to leucine-devoid diets, tunicamycin-induced ER stress, poly(I)poly(C) nucleotide which mimics viral stress, and sodium arsenite which induces oxidative stress. Luminescence and ATF4 protein levels correlated with phosphorylated eIF2 [53]. Mouse embryonic fibroblasts (MEFs) in a leucine-free medium supplemented with various levels of leucine (from .01 up to .8 mM) showed reduced luciferase activity in a dose-dependent manner. MEFs transferred from normal to leucine-free medium showed steadily increasing luciferase activity over time (1, 2, 4, 6, 8 h), and MEFs transferred from leucine-free to normal medium showed steadily decreasing luciferase activity [53].

Notably, in a comparison of the luminescence in *ex vivo* liver, kidney, pancreas, spleen, heart, lung, muscle, and brain, leucine deprivation differed from control only in liver [53]. The increase in luminescence during leucine deprivation denotes translation of the *Atf4* gene during stress, and tissue specific differences in luminescence indicate differing levels of activity of the ISR. The increase in hepatic luminescence suggests that the liver launches an intensive ISR during amino acid stress, which is not seen in other tissues. Although ATF4 is expressed in many other tissues, its hepatic induction may be the most important to investigate.

These findings correspond well with the published literature, where many effects of amino acid deprivation or restriction in the liver have been noted. Hepatic effects include reduced protein synthesis [29]; reduced triglyceride content [18, 29]; increased expression of *Fgf21* [11]; and protection from pharmacological [22] and diet induced [29] steatosis. Hepatic ATF4, specifically, is necessary for increased serum FGF21 and phenotypic effects [11] and the effects of asparagine deprivation in liver differ from those in MEFS [11]. The number and variety of hepatic effects, and the observation of tissue-specific differences in response to SAAR, provide evidence along with the UMAI model that not only is translation of ATF4 a hallmark of the ISR, but its effects in the liver may be needed for many outcomes.

FGF21: an ISR "mediator"

Many physiological outcomes of protein and amino acid deprivation and restriction appear mediated through the ATF4 target Fibroblast Growth Hormone 21 (FGF21). FGF21 is a nutritionally regulated hepatokine, and its elevation during SAAR corresponds with effects on food intake, energy expenditure, hepatic lipid metabolism, and body composition [50]. ATF4 increases hepatic gene expression of *Fgf21* during amino acid stress [49]. It is presupposed that improvements in body composition and energy expenditure, without decreased food intake, may result from the ISR in part through an ATF4-FGF21 axis.

FGF21 is a member of the endocrine subfamily of FGFs which includes FGF19 and FGF23. These particular FGFs are unique in that they bind heparin poorly, unlike other FGFs, and act as classical endocrine hormones (an action which requires the presence of Beta-Klotho protein and Klotho co-receptor in their target tissues) [54, 55]. Although primarily a hepatokine, FGF21 is expressed to lesser extents in muscle and adipose tissue, as well as the gut, brain, heart, and pancreas.

As an ATF4 target gene, it has two AARE/CAREs, starting at positions -152 and -610 upstream of the transcription start site [49]. Both cis-elements bind ATF4, and the first is essential for *Fgf21* induction [49]. In addition to total amino acid deprivation [49], enhanced recruitment of ATF4 and RNA polymerase II to the *Fgf21* promoter has been seen in the case of single amino acid deprivation, such as alanine [56]. FGF21 can also be induced through the binding of the transcription factor X box binding protein (XBP1) to an ER stress response element (ERSE) [57]. This suggests a possible route for ATF4-

independent elevation of FGF21, but other investigators have found elevated FGF21 during ER stress to be ATF4 dependent [58], and siRNA-mediated interference of *Atf4* during amino acid stress significantly diminishes the increase in *Fgf21* mRNA levels in HepG2 cells [49]. In addition to CARE and ERSE, the *Fgf21* promoter also has response elements for carbohydrates, peroxisome proliferator-activated receptors (PPARs), and glucagon [59].

There has been some confusion in the literature as to what conditions elevated FGF21 represents. Initial investigations found FGF21 to be elevated, paradoxically, by both overfeeding and fasting [59]. It has been hypothesized that high fat contributes to increases in FGF21 during a ketogenic diet [60]; in contradiction to that hypothesis, FGF21 also increases during starvation [61]. A geometric framework of 25 different diets, comprising various manipulations of macronutrients and energy, clarified FGF21's role as a signal of protein restriction (PR) [62].

Although FGF21 is elevated during both conditions of overfeeding and starvation, amino acid restriction within these disparate nutritional contexts seems to be the true trigger of increased FGF21. This aligns with *Fgf21's* status as a target of ATF4, which is translated during conditions of amino acid stress, including SAAR. Protein restriction is the only condition to increase serum FGF21 consistently regardless of other macronutrient levels [62]. Reduced protein intake positively correlates with increased serum FGF21, unlike fat or energy, which show no association [62]. A smaller reduction in protein is also able to evoke greater responses in FGF21 when coupled to higher carbohydrate, synergism

which is not seen for other macronutrients [62]. Restricting protein is also more effective than restricting calories at increasing hepatic FGF21 expression and serum levels (with no increase in expression in white epidydimal adipose tissue or muscle) within 4 days in rats [63]. In fact, CR alone *reduced* serum FGF21 levels, and combined PR and CR resulted in FGF21 levels greater than control but less than PR alone [62]. FGF21 was also increased more by leucine deprivation, rather than starvation, in HepG2 cells [62]. Although protein restriction is often an in-built effect of cutting calories, experimental designs which isolate their effects show that FGF21 responds sensitively to fluctuations in amino acid availability.

As a nutritionally regulated hormone, FGF21 exerts effects on a whole-body level, particularly through altering metabolism, with positive effects not unlike PR and SAAR on health and in many disease states [64-67]. In fact, FGF21was first identified not through a nutritional study but by a pharmaceutical screen. This marked it as a ‘metabolic regulator’; its administration for two weeks in a model of diet induced obesity led to a 6% reduction in adiposity without decreased food intake [68]. Energy expenditure was significantly increased during both dark and light periods, as well as core body temperature. These effects of exogenous administration are seen not only in genetic [68] but also in dietary [69] models of obesity. Correlations between FGF21 levels and improved body composition and increased energy expenditure were also observed in a genetic model of alanine depletion [56]. FGF21 administration was further found to attenuate hepatic fibrogenesis [70] and reverse steatosis [69]. These findings provide a

foundation for the hypothesis that effects of ATF4 and the ISR during amino acid stress are mediated through FGF21.

Because many studies of FGF21 use models of exogenous pharmacological administration, it is important to confirm whether physiological changes in FGF21 levels which occur *in vivo* are sufficient. To address this point, Wanders et al examined FGF21 levels during SAAR in wild type and *Fgf21* KO mice [51]. Their use of the *Fgf21* KO mouse model provides additional insight to the literature investigating exogenous administration or correlated changes in serum levels.

The findings of *Fgf21* KO studies are consistent with exogenous administration, in that changes in food intake and energy expenditure are regulated in response to diet by physiological changes in serum FGF21. Not only did *Fgf21* KO prevent the SAAR-induced hyperphagy seen in WT mice, but it reduced food consumption basally [51]. Wild type mice showed a significant increase in energy expenditure by day 6 of a SAAR diet compared to control, which remained at 8 weeks [51]. *Fgf21* KO mice did not increase energy expenditure at any point [51].

Fgf21 KO studies also reveal FGF21 independent responses to SAAR. After 4 weeks of a high fat diet, 4 weeks of SAAR *reversed* body weight gain and fat accumulation in both wild type and *Fgf21* KO mice [51]. Changes in hepatic gene expression during SAAR were seen in *Fgf21* KO mice in the same direction but at lesser magnitudes. SAAR decreased hepatic *Scd1* expression in both wild type and *Fgf21* KO mice, but the decrease

was less in *Fgf21* KO than in wild type mice [51]. Compared to control, SAAR induced significantly less expression of several Nrf2 targets in *Fgf21* KO mice than wild type (*Gsta2*, *Mgst3*, *Psat1*) with one exception, *Nqo1*, induced more during SAAR in *Fgf21* KO [51]. *Asns*, another ATF4 target gene, was induced by SAAR in both genotypes although to a lesser extent in *Fgf21* KO [51]. Oppositely, ATF4 target gene *Vldr* was induced more by SAAR in *Fgf21* KO mice than in wild type [51].

These findings suggest that FGF21 is needed for SAAR-induced alterations in energy intake and expenditure, as well as for the full extent of characteristic changes in gene expression. They point to a disconnection between FGF21 and changes in body composition which merits closer inspection. FGF21 drives mice to eat more, and to expend more energy while doing so, but the improvement in body composition seen after SAAR in *Fgf21* KO mice shows that FGF21 is not required for this effect. It also shows that improvement in body composition is not only the result of increased energy expenditure, as increased energy expenditure did not occur in *Fgf21* KO mice. These findings both clarify our understanding and add complexity to our view of FGF21's role in SAAR and highlight the need for further study.

Does the ISR sense and respond to SAAR?

Although ATF4 synthesis during amino acid stress results from eIF2 phosphorylation by GCN2 [27], there is also evidence that ATF4 translation may be initiated regardless of *Gcn2* status [28, 71, 72], and of phenotypic changes during SAAR that are GCN2

independent [10, 52]. Further, some changes in gene expression during ER stress, which is included under the umbrella of stresses sensed by the ISR, are ATF4 independent [11] and the effect of ATF4 on metabolism contradicts expectations [73-76]. These data collectively challenge the concept that SAAR is necessarily sensed by and responded to via the pathway traditionally known as the ISR. It may be that a modification to the schema is required, or that an entirely new one must be drawn. Depicting all relationships that have emerged from the recent literature leads to a branching web more than a linear response. Only GCN2-independent TC is added to the ISR in Illustration 1, but the details of more recent investigations are discussed below.

SAAR does not rely solely on GCN2 for recognition. In both *Gcn2* KO and wild type mice fed SAAR, phosphorylation of hepatic eIF2 was increased four- to five-fold at 6 days and 14 weeks [71]. However, *Gcn2* KO and wild type mice showed changes in hepatic gene expression characteristic of NRF2, which is activated by GCN2's sister enzyme PERK [71]. Importantly, there were no changes in genetic markers of ER stress, which PERK is canonically a sensor of as part of the ISR [71]. This raises the possibility of crossover among the kinase "sensors" of the ISR. Yet kinase crossover cannot explain all instances of anomalous *Atf4* expression. *Atf4* expression was also GCN2 independent during methionine deprivation (MD) in MEFs, although expression was much lower in cells lacking *Gcn2* [72]. Ruling out the possibility of PERK rescuing eIF2 phosphorylation, MEFs with non-phosphorylable eIF2 increased *Atf4* expression during MD [72]. The level of *Atf4* expression was admittedly lower than that seen in wild type MEFs, and it was also triggered by deprivation of methionine and not of leucine [72].

Overall, these data suggest that ATF4 is translated to some extent and in some conditions independently of the GCN2-eIF2 axis.

SAAR does not rely solely on phosphorylation of eIF2 to effect translation control. Pettit et al [28] found increased eIF2 phosphorylation in wild type, but not *Gcn2* KO, mice following 5 weeks of SAAR; but that despite the GCN2-dependence of eIF2 phosphorylation, *Gcn2* KO mice were still responsive to SAAR in several measures. Activity of EIF2B, the guanine exchange factor critical for 'refreshing' the competent translational complex, decreased, suggesting translational control was in effect [28]. Expression of ISR related genes was increased [28]. In accordance with an active ISR, which reduces global translation to conserve cellular resources, the protein synthetic rate (as measured using deuterium enrichment of alanine into tissue proteins) was reduced in cytosolic and mixed but not mitochondrial fractions in liver and skeletal muscle [28]. This corroborates the phospho-eIF2 independent increase in ATF4 seen in *Gcn2* KO MEFs [72], and again suggests an alternative to the canonical sensor-core-effector relationship of the ISR.

SAAR does still seem to require ATF4. Laeger et al described a GCN2-independent pathway for PR with a delayed increase in ATF4 and FGF21 [10]. Loss of GCN2 impaired the acute response to PR, with no change in fat or lean mass or hepatic gene expression within 2 weeks [10]. The increase in serum FGF21 in *Gcn2* KO mice was also significantly less than that in wild type mice fed PR diet [10]. However, by 3 weeks PR *Gcn2* KO mice were gaining significantly less weight than their controls, and by 11

weeks their energy expenditure was increased [10]. The increase in circulating FGF21 at 27 weeks in PR *Gcn2* KO mice was significantly greater than at 2 weeks, as well as binding of ATF4 to the *Fgf21* promoter [10]. PR *Fgf21* KO mice were not different from their controls at any time [10]. These results show that ATF4 drives FGF21 expression during amino acid stress, and this FGF21 expression is required for changes in body composition, energy expenditure, and hepatic gene expression. While driven by GCN2 acutely, some compensatory mechanism steps up to increase ATF4 and FGF21 during chronic amino acid stress.

An independent role for ATF4 is supported by global RNA sequencing data from our lab investigating livers of amino acid depleted (asparaginase treated) wild type *Gcn2* KO and *Atf4* KO mice [52]. We found overlapping pathways between GCN2 and ATF4, as well as GCN2-independent pathways regulated by ATF4 [52]. Seen only in *Gcn2* KO were alterations in p38 MAPK signaling, steroid hormone biosynthesis, growth arrest, and DNA damage pathways [52]. Seen only in *Atf4* KO were changes in cytochrome p450 mediated processes and oxidative phosphorylation pathways [52]. These findings show that not all effects of ATF4 rely on GCN2.

The portrayal of an ISR which *requires* ATF4 is complicated by the literature. Despite its clear importance during stress, surprisingly ATF4-independent responses are reported. ATF4-independent CCAAT-enhancer-binding protein homologous protein (CHOP) mRNA expression is seen in ER stressed Hepa1-6 cells, as well as full induction of CHOP protein [11]. This was driven by ATF6, expression of which was also ATF4-

independent [11]. Not all ISR outcomes depend on ATF4, but some outcomes may. FGF21 remained ATF4 dependent, and knocking out *Atf4* only in the liver was sufficient to reduce the increase in FGF21 during ER stress [11].

Studies done with *Atf4* KO mice report perplexing metabolic changes. Because ATF4 increases FGF21, which is required for increased energy expenditure during PR [10], it is surprising that *Atf4* KO mice show a hypermetabolic phenotype basally[73] and during cold stress [74]. *Atf4* KO in agouti-related protein AgRP [75] and pro-opiomelanocortin (POMC) [76] neurons was also reported to increase energy expenditure basally [75, 76]. Whether such increases in energy expenditure were associated with FGF21 was not examined, although changes in lipid metabolism in adipose tissues [73] which resemble effects of FGF21 during amino acid starvation [77] were observed. What role ATF4 plays in SAAR's hypermetabolic phenotype, and whether it indicates an uncoupling of ATF4 and FGF21, remains uncertain.

Considering the ATF4-independent induction of ER stress response genes [11], the ATF4-dependent but GCN2-independent changes in gene expression during asparaginase treatment [52], and GCN2-independent but FGF21-dependent responses to SAAR [10], more work characterizing the role of ATF4 during SAAR remains to be done. ATF4 may be essential for certain responses to SAAR, albeit not via GCN2 [28]. Relatively acute changes in food intake, body composition, energy expenditure, hepatic gene expression, and FGF21 may require ATF4. At the same time, there is the possibility that some of these effects are mediated by other, ATF4-independent translation factors, as seen with

CHOP induction by ATF6 during ER stress [11]. To address whether ATF4 is necessary for increased or maintained food intake, improved body composition, increased energy expenditure, and changes in hepatic gene expression and FGF21 in response to SAAR, we investigated the effect of *Atf4* KO in mice.

The **hypothesis** of this work is that ATF4 is required for changes in feeding behavior, energy expenditure, body composition and hepatic gene expression during SAAR; and that hepatic expression of *Fgf21* is both ATF4 dependent and associated with phenotypic effects.

It is expected that a high fat SAAR diet for 5 weeks will increase food and fluid intake and energy expenditure in wild type mice, improve their body composition, and lead to increased expression of *Atf4* as well as ATF4 targets in the liver, most notably *Fgf21*. Loss of *Atf4* should prevent these effects, such that a high fat SAAR diet for 5 weeks will not increase food intake or energy expenditure, improve body composition, or lead to increased expression of ATF4 targets in liver such as *Fgf21*. Levels of hepatic *Fgf21* expression will be related to changes in food and fluid intake, energy expenditure, and body composition.

The specific **aims** of this work are

- To determine whether ATF4 is needed to increase food and fluid intake and energy expenditure, improve body composition, and alter hepatic gene expression during SAAR

- To determine whether elevated *Fgf21* during SAAR is ATF4-dependent and related to SAAR-induced increases in food and fluid intake and energy expenditure, and improvements in body composition

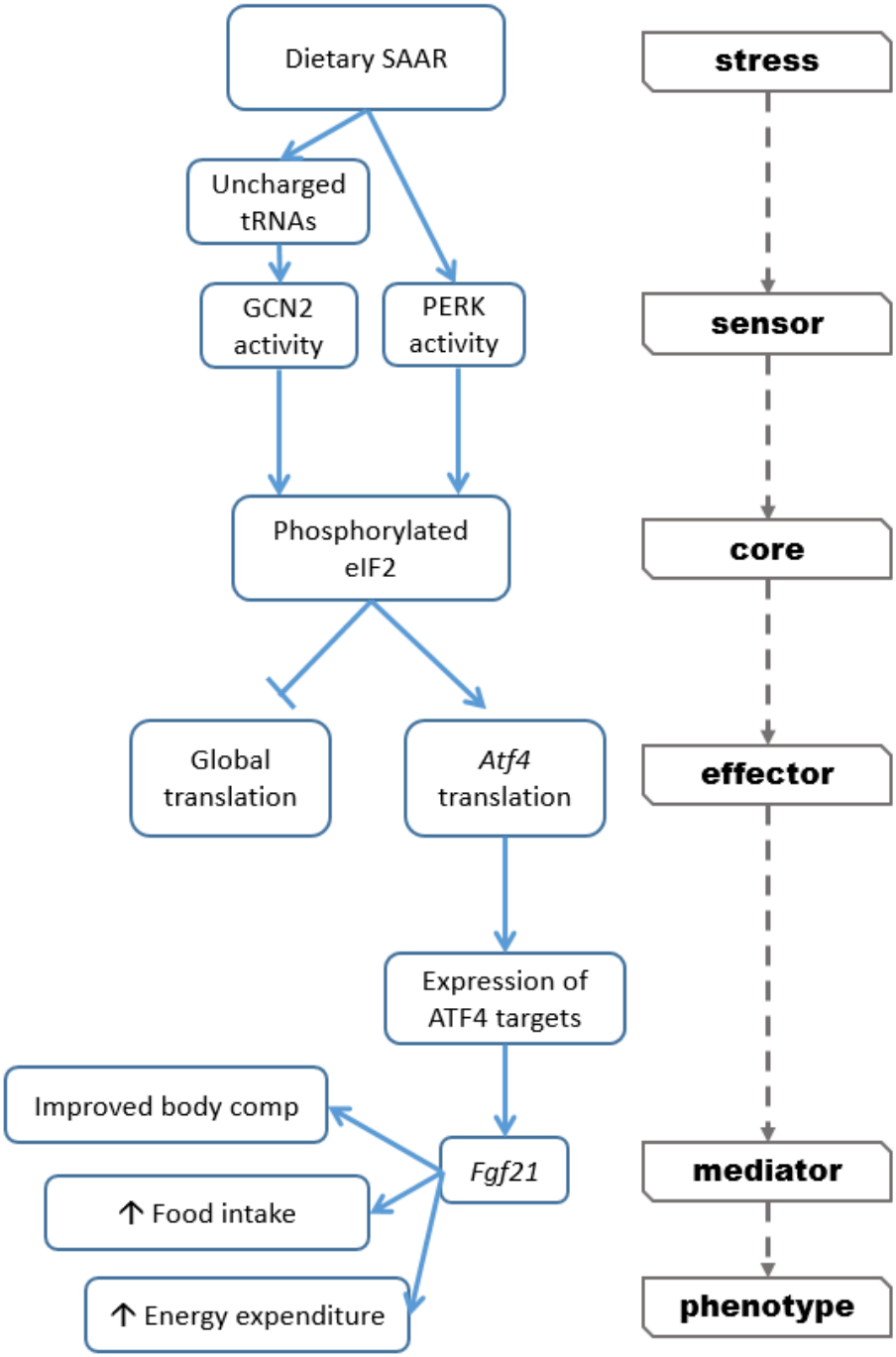

Illustration 1. Representation of the ISR during SAAR. Accumulation of uncharged tRNAs during dietary SAAR activates GCN2, leading to translational control via phosphorylation of eIF2. In addition to GCN2 activity, PERK is able to increase eIF2 phosphorylation during SAAR. Phosphorylation of eIF2, the core mechanism of this pathway, favors gene-specific translation of ATF4. ATF4 is an effector of the ISR, and functions as a transcription factor promoting adaptive gene expression. ATF4 transcriptional targets, such as *Fgf21*, mediate physiological and behavioral changes which result in a whole-body phenotype.

Chapter 2: The effect of *Atf4* in Dietary Sulfur Amino Acid Restriction

Introduction

Caloric and protein restriction improve body composition, which is an important aspect of preventing degenerative disease. Reduced percentage of body fat is accomplished despite increased caloric intake – not less – in the case of protein restriction [1, 3]. Altering protein composition at the level of individual amino acids offers the same benefit, with restriction of sulfur amino acids creating a whole-body phenotype characterized by increased food intake, increased energy expenditure, and reduced adiposity as well as numerous health benefits [9, 12, 14-16, 18, 22-24, 26, 50]. It is unclear to what extent the mechanisms sensing protein restriction are involved in sensing SAAR. Among the mechanisms identified, the ISR may contribute importantly based on its activation by amino acid stress [27, 29-32, 34, 37]. Activation of the ISR promotes selective translation of ATF4 to initiate adaptive gene expression during a variety of stresses including amino acid deficiency [11, 48, 49, 52, 53]. One notable ATF4 target, FGF21, is necessary for SAAR's effects [51] and by itself is sufficient to increase food intake and energy expenditure while reducing body fat when exogenously administered [68, 69]. Recently, both low protein diets and exogenous FGF21 administration have been shown to increase water consumption [78]. To determine whether *Atf4* is necessary for SAAR to increase food and water intake, energy expenditure, and reduce adiposity, male and female mice were treated for 5 weeks with a high fat SAAR or high fat control diet.

Methods

Animal protocol:

All animal procedures and protocols were reviewed and approved by the Rutgers University Institutional Animal Care and Use Committee. Mice were located in the Bartlett Animal Facility on Cook Campus and maintained on a 12 hour light-dark cycle at 24 degrees Celsius, with 40% daily average humidity. Before assignment to experimental diets, mice were provided unlimited access to commercial chow (LabDietRodent 5001) and tap water. All mice were housed in solid-bottomed clear plastic cages with soft bedding and were provided environmental enrichment.

C57BL/6J *Atf4*$^{-/-}$ (Jackson Labs) were bred at the Bartlett Animal Facility, with *Atf4*$^{+/+}$ littermates kept as wild type controls. C57BL/6J *Atf4*$^{-/-}$ bred poorly; so in an effort to improve reproduction, male C57BL/6J *Atf4*$^{-/+}$ were outbred one generation to female Swiss Webster mice. Progeny from F1 and F2 generations were included in the study.

Diets and experimental design:

Atf4$^{+/+}$ wild type (WT) and *Atf4*$^{-/-}$ knock out (KO) mice were single housed into clear, solid-bottomed plastic cages with soft bedding and were provided environmental enrichment. At 18-20 weeks of age, WT and KO mice were placed on a high fat (60% fat by kcal) zero cysteine control diet (CON). Mice were acclimated to CON for one week and then randomly assigned by weight to either remain on CON (Female *Atf4*$^{+/+}$ n=3, *Atf4*$^{-/-}$ n=5; male *Atf4*$^{+/+}$ n=4, *Atf4*$^{-/-}$ n=3), or switch to a high fat SAAR (.12% Met, 0%

Cys) diet (Female *Atf4*$^{+/+}$ n=7, *Atf4*$^{-/-}$ n=7; male *Atf4*$^{+/+}$ n=11, *Atf4*$^{-/-}$ n=5). Both diets were isocaloric (5.3 kcal/g) and isonitrogenous, as previously described by Pettit et al [28]. Experimental feeding period was 5 weeks.

Body weight and food intake were measured daily throughout the study, and body composition was assessed weekly using MRI (EchoMRI). At the end of 5 weeks, mice were monitored in a Comprehensive Lab Animal Monitoring System (CLAMS, Columbus Instruments) for 2-5 days. Several days after metabolic phenotyping, mice were euthanized by guillotine decapitation. Trunk blood was collected from the neck and allowed to clot on ice before centrifuging at 2,000 rcf for 15 minutes to collect serum. Liver, kidney, gonadal and subcutaneous fat, gastrocnemius and soleus muscle, heart, spleen and brain were dissected on ice and then weighed, foil-wrapped and flash frozen in liquid nitrogen before storage in a -80ºC freezer.

MRI:

Lean calibration was performed at the time of manufacture using chicken breast 35, and fat calibration was performed before each scan using canola oil. Mice were secured in clear acrylic tubes just tightly enough to prevent turning around. Accumulation was set to 3, and mice were scanned until at least two fat readings were within 0.2 grams of each other.

Metabolic phenotyping:

Measurements were taken every 4-12 minutes per cage. O_2 consumption (VO_2) and CO_2 production (VCO_2) were determined; RER was calculated for each mouse as the ratio of VCO_2 / VO_2.

The instrument's "Internal" method (Oxymax Hardware Manual 0233-002M, p 31) reports whole-body energy expenditure by multiplying VO_2 with a calorific value (CV) derived from observed RER: CV = 3.815 + 1.232 * RER ; whole body energy expenditure = CV * VO_2. This was normalized using lean mass obtained by MRI at the start of metabolic phenotyping[78].

Because time between gas exchange measurements varied between cohorts, calculated energy expenditures from output containing more frequent measurements (up to every 4 minutes) were averaged, aligning them with output containing less frequent measurements (once every 12 minutes). Aligned data was used to create group averages at each time point for visualization of diurnal patterns. To improve readability, the smooth.spline function in R was used to fit a cubic smoothing spline to time series data. This created a flexible and nonlinear model which followed the original data closely but reduced some of the noise.

Gene Expression:

RNA isolation: Tissues were pulverized by liquid-N_2-cooled mortar and pestle and 0.01 g of each sample was homogenized in 1 mL of TRIzol (Molecular Research Center) with a

Polytron. Homogenized samples were vortexed with 100 µL bromoanisole for phase separation and centrifuged for 15 min at 12,000 relative centrifugal force (rcf). 500 µL of supernatant was collected and precipitated overnight at -20º C with equal volume isopropanol and then centrifuged 20 min at 12,000 rcf to pellet. Pellets were washed 3 times by addition of 1 mL 70% ethanol and 5 minutes centrifugation at 7500 rcf. RNA stock was created by resuspending the pellet in 30 µL of nuclease free water (NFW), and a working solution was created by pipetting 1.5 µL RNA stock into 99 µL NFW, and both stored at -80º C.

RNA quality and concentration were assessed using a Nanodrop fluorospectrometer (Thermo Fischer Scientific). Clear, strong absorbance peaks at 260 nm, minimal or no shoulder at 230 nm, and 260:280 absorbance ratios of 1.8-2 were considered acceptable. Concentration measurements were used to dilute 1 µg RNA into 10 µL NFW.

cDNA synthesis: cDNA was synthesized with a high capacity cDNA reverse transcriptase kit (Life Technologies), using 1 µg of RNA per reaction.

Reverse-Transcription quantitative PCR (RTqPCR): RTqPCR was conducted using TaqMan Fast Universal PCR Mastermix (Applied Biosystems) according to manufacturer instructions, with cDNA diluted 1:20. Primers were validated using serial dilutions of cDNA made from a pooled RNA sample. Threshold cycle (C_T) was plotted against sample concentration, and $R^2 > .98$ was considered acceptable.

Amplification and detection were carried out in a StepOne real-time PCR system (Applied Biosystems). Each sample was run in triplicate, and each 96-well plate included one water blank, one no-template and one no-reverse transcriptase control.

Gene expression: GAPDH was used as a housekeeping gene. C_Ts were not different between groups, confirming that GAPDH expression was not altered by treatment. ΔC_Ts were calculated as C_T GAPDH – C_T Gene of Interest (GOI) for each animal. $\Delta\Delta C_T$s were calculated as [average ΔC_T of WT CON group] – ΔC_T of each animal. Relative mRNA quantity (RQ) was calculated as $2^{\Delta\Delta CT}$ for each animal. All RQ values were divided by the average RQ of the WT CON group for presentation with the control group average = 1. Statistical analysis was performed on log transformed data.

Statistical Analysis:

Data are presented with group means +/- SD. Approximately normal distribution was confirmed by the Shapiro-Wilkes test, and homogeneity of variances by Levene's test. The null hypothesis of equal group means was tested using an analysis of variance (ANOVA). A significant effect was considered $p < 0.05$, and in the case of interaction effects, post-hoc analysis was performed using Tukey's Honestly Significant Differences (HSD) test to control for multiple comparisons. Computations were performed with STATISTICA. Graphs were created using Prism version 6 (GraphPad Software) and the DescTools package for R.

Results

Body weight:

At two weeks of treatment following one week of acclimation (week 3 in Figure 1), there was a main effect of diet by which SAAR reduced BW, despite the diet containing 60% fat by kcal. By the second week of treatment, average BW in WT CON mice remained level but the average BW of WT SAAR mice decreased visibly, with a much smaller decrease visible in KO SAAR mice. At three weeks of treatment (week 4 in figure 1) a significant strain-diet interaction appeared which remained for the rest of the study. WT CON mice had significantly greater BW than all other groups, including WT SAAR, KO CON and KO SAAR. WT SAAR mice had significantly greater BW than KO mice, including KO CON and KO SAAR. There was no significant difference between KO CON and KO SAAR (Figure 1). SAAR was effective in reducing BW in WT mice, but not in KO mice.

Food intake:

Daily food intake per gram body weight in WT SAAR and KO SAAR females appeared visibly higher after just one week of treatment (week 2 in Figure 2, Females), but this difference was not statistically significant. The gap between WT SAAR and WT CON females remained consistent during the 5 week treatment period, while the gap between KO SAAR and KO CON females was not consistent due to fluctuations in KO SAAR intake.

Food intake per gram body weight in KO females was generally higher than in WT females, and this difference was confirmed as a main effect of strain in treatment weeks one, three and four (weeks 2, 4 and 5 in Figure 1, Females). In the final, fifth week of the study, a strain-diet interaction appeared, but post hoc comparisons were not significant (week 6 in Figure 2, Females).

Daily food intake per gram body weight in WT SAAR males appeared visibly higher after one week of treatment (week 2 Figure 2, Males). Intake in KO CON and KO SAAR males fluctuated over the 5 week treatment period. After one week of treatment, WT SAAR, KO CON and KO SAAR males had similar average food intakes. After two weeks of treatment, average food intake in KO SAAR was numerically highest, followed by WT SAAR, with lowest average food intake in KO CON and WT CON. The relationship between KO CON and KO SAAR was reversed at three weeks of treatment, with WT SAAR and KO CON having numerically higher average food intake than WT CON and KO SAAR. At four weeks of treatment, although WT SAAR intake was similar to the previous three weeks and numerically higher than WT CON, the average food intakes of KO CON and KO SAAR mice were both indistinguishable and intermediate between WT SAAR and WT CON. There was a trending effect of diet $p<.1$ with SAAR > CON during the third and fourth weeks of treatment (weeks 4 and 5, Figure 2, Males). At five weeks of treatment (week 6 Figure 2, Males) there was a significant main effect of diet, with SAAR > CON.

Examination of the individual values of daily food intake per gram body weight in female mice during the final, fifth week of treatment shows that food intake was higher in almost all WT SAAR females than in WT CON females, but by a relatively small amount of less than five-tenths of a gram of food per gram BW (Figure 3, Females). This difference was not statistically significant. The distribution of food intakes in KO CON and KO SAAR mice appeared very similar to each other and to WT SAAR. The only effect by two-way ANOVA in females was a trending effect of strain $p<.1$, with KO > WT (Figure 3, Females).

Examination of individual values of daily food intake per gram body weight in male mice during the final, fifth week of treatment shows that food intake was higher in almost all WT SAAR males than in WT CON males, often by more than five-tenths of a gram food per gram BW (Figure 3, Males). The distribution of food intakes in KO CON and KO SAAR were similar to each other, with one value of food intake in KO SAAR appearing higher than the cluster of values in KO CON (Figure 3, Males). There was a main effect of diet in males $p<.05$, indicating that SAAR significantly increased daily weight-specific food intake in both WT and KO male mice, although not in females.

Body composition:

Percent body fat after one week of acclimation to CON and percent body fat after 5 weeks of treatment in mice of a Swiss Webster background were compared in each group

using two-tailed, paired T-Tests (Figure 4 and Table 1). Over the 5 week treatment period, adiposity significantly increased in WT CON, KO CON and KO SAAR males and females $p<.05$ (Figure 4 and Table 1). Despite consuming a high fat, 60% fat by kcal diet for 5 weeks, percent body fat was not significantly different in WT SAAR (Figure 4 and Table 1). Examining paired data shows that of all WT SAAR males and females, n=13, only one showed an upward trend in adiposity (Figure 4). In comparison, paired data for KO SAAR, n=9, showed several strong upward trajectories (Figure 4). SAAR is able to effectively protect WT mice from increased adiposity on a high fat diet, but it is not able to protect KO (Figure 4 and Table 1).

Change in percent body fat over the 5 week treatment period was compared between groups and sexes (Figure 5). In females, all groups had positive average changes in adiposity (Figure 5, Females). In males, WT CON, KO CON and KO SAAR had positive average changes in adiposity while WT SAAR had a negative change in adiposity (Figure 5, Males). MANOVA of change in percent body fat with sex, strain and diet as factors showed a significant sex-strain-diet interaction. Change in adiposity in WT SAAR males was significantly lower than WT CON males $p<.001$ and all females $p<.01$ (Figure 5). There was no difference between female WT CON, WT SAAR, KO CON or KO SAAR, male KO CON and male KO SAAR (Figure 5).

Water intake and energy expenditure:

After 5 weeks of treatment mice were metabolically phenotyped in a Comprehensive Lab Animal Monitoring system, which included measurements of water intake (Figure 6). Water intake per gram BW, summed over 48 hours, in WT SAAR males and females clustered clearly above WT CON (Figure 6). WT CON, KO CON and KO SAAR water intakes clustered closely together, with several KO SAAR intakes slightly higher than KO CON (Figure 6). Two way ANOVA revealed a main effect of diet $p<.05$, showing that SAAR significantly increases water intake in WT and KO mice (Figure 6).

Energy expenditure as kcal/hr per gram lean mass over 48 hours was shifted upward in SAAR males (Figure 7). Energy expenditure was visibly higher in WT SAAR than in WT CON males, and higher in KO SAAR than in KO CON males, during both the dark and light periods (Figure 7). Interestingly, energy expenditure followed a regular diurnal rhythm in WT males but appeared arrhythmic in KO males (Figure 7). For males, the 12-hour average of energy expenditure as kcal/hr per gram lean mass during the dark and light periods for WT SAAR clustered clearly above WT CON, and KO SAAR also appeared slightly higher than KO CON. ANCOVA of kcal/hr with lean mass as a covariate revealed a main effect of diet $p<.001$, showing that SAAR increased energy expenditure in WT and KO males (Figure 8).

Energy expenditure as kcal/hr per gram lean mass over 48 hours was not shifted upward in SAAR females (Figure 9). Energy expenditure was not visibly higher in WT SAAR than in WT CON females, or in KO SAAR than KO CON females (Figure 9), in either

the light or dark periods. Energy expenditure follows a regular diurnal rhythm in WT and KO females, but appears dampened in KO females (Figure 9). For females, the 12-hour average of energy expenditure as kcal/hr per gram lean mass during the dark and light periods of WT CON, WT SAAR, KO CON and KO SAAR clustered near each other (Figure 10). ANCOVA of kcal/hr with lean mass as a covariate revealed no effects of strain or diet, showing that SAAR does not increase energy expenditure in WT or KO females (Figure 10).

SAAR's influence on energy expenditure in males, but not females (Figures 7-10) was seen as a statistically significant sex-diet interaction in ANCOVA of kcal/hr performed with grams lean mass as a covariate (Figure 11). SAAR males had higher energy expenditure than CON males, while SAAR females did not have higher energy expenditure than CON females (Figure 11). Average energy expenditure in CON and SAAR females was numerically similar to SAAR males, and higher than CON males. Post hoc comparisons show male SAAR > male CON, female CON and female SAAR $p<.001$ (Figure 11).

The influence of KO on diurnal fluctuations in energy expenditure (Figures 7 and 9) was seen as a statistically significant strain-period interaction in ANCOVA of kcal/hr performed with grams lean mass as a covariate (Figure 12). WT mice had higher energy expenditure during the dark period than during the light period, while KO mice did not. Energy expenditure in KO mice was significantly higher than WT during the light period

(when energy expenditure is normally low) and significantly lower than WT during the dark period (when energy expenditure is normally high). Post hoc comparisons show WT dark > WT light, KO dark, and KO light $p < .001$ and KO light > WT light $p < .01$.

Tissue weights:

After 5 weeks of treatment, tissue weights were collected (Table 2). MANOVA with sex, strain and diet as factors was performed on liver, gonadal fat, subcutaneous fat, heat, gastrocnemius, soleus, kidney, spleen and brain weights per gram BW. There were no significant differences in BW-normalized liver, heart, gastrocnemius, soleus, kidney, or spleen weights (Table 2).

There was significant strain-diet interaction in BW normalized gonadal fat weights (Table 2). Post hoc comparisons show that grams of gonadal fat per gram BW were higher in WT CON than in WT SAAR, KO CON and KO SAAR $p < .001$ (Table 2). There was significant sex-diet-strain interaction in subcutaneous fat weights (Table 2). Post hoc comparisons show that grams of subcutaneous fat per gram BW were higher in male WT CON than female WT CON, WT SAAR, KO CON and KO SAAR, as well as higher than male WT SAAR, KO CON and KO SAAR $p < .05$ (Table 2). There was also an effect of strain in brain weight per gram BW, which was higher in KO mice (Table 2).

Gene expression:

Hepatic *Atf4* expression after 5 weeks of treatment was increased by SAAR in females and males. Hepatic expression of *Atf4* in KO males and females was negligible, with average mRNA Relative Quantity around .1, compared to expression in WT CON which was set to 1 (Figure 13). MANOVA performed on log transformed data with sex, strain and diet as factors shows an effect of strain $p<.000001$, and effect of diet $p<.05$ (Figure 13). Another ISR effector is *Atf5*, which is regulated by PERK-mediated phosphorylation of eIF2 during ER stress as part of the unfolded protein response [79]. In response to SAAR, hepatic *Atf5* expression was not increased (Figure 14). MANOVA on log transformed data showed that hepatic *Atf5* expression was unaffected by KO, or by sex (Figure 14).

Hepatic expression of *Fgf21* was elevated by SAAR in WT and KO males and females (Figure 15). *Fgf21* expression was numerically higher in SAAR males than females. MANOVA on log transformed data showed no significant effect of sex. *Fgf21* expression was basally elevated in KO, in both males and females, with a main effect of strain $p<.05$ (Figure 15).

Hepatic expression of *Nuclear protein 1*, or *Nupr1*, was increased by SAAR in WT males and females, but not in KO (Figure 16). *Nupr1*, also known as p8, was originally identified as a gene induced during pancreatitis [80]; it has since been identified in numerous other settings[81-85] including ER stress [86], oxidative stress [80], amino acid starvation [87], and dietary protein dilution [88]. The GCN2/ATF4 pathway was

found to regulate *Nupr1* through an AARE [87]; *Nupr1* expression is promoted by C/EBP-beta trans-acting factors [89]; and *Atf4* overexpression increased *Nupr1* expression, while siRNA-mediated loss of *Atf4* diminished it [90].

MANOVA on log transformed data showed was an effect of diet and strain-diet interaction in hepatic *Nupr1* expression, with WT SAAR > WT CON but no significant differences between KO CON and KO SAAR (Figure 16). *Nupr1* expression in KO CON and KO SAAR females ranged from as low as WT CON to as high as WT SAAR (Figure 16, Females). *Nupr1* expression in KO SAAR males clustered with KO CON and WT CON males, but *Nupr1* expression in several KO SAAR males was at the level of WT SAAR males (Figure 16, Males). There was also a main effect of sex $p<.01$, with Females > Males $p<.05$ (Figure 16).

Hepatic expression of *Stearoyl coenzyme A desaturase 1*, or *Scd1*, was not significantly affected by SAAR, but was reduced in KO males and females (Figure 17). *Scd1* catalyzes a rate limiting step in lipid synthesis, and reduction in its expression and activity are associated with leanness [6]. The reduction of *Scd1* expression in KO males was numerically greater than the reduction in females (Figure 17). MANOVA of log-transformed *Scd1* expression with sex, strain and diet as factors shows significant effect of strain $p<.05$ (Figure 17).

Figures

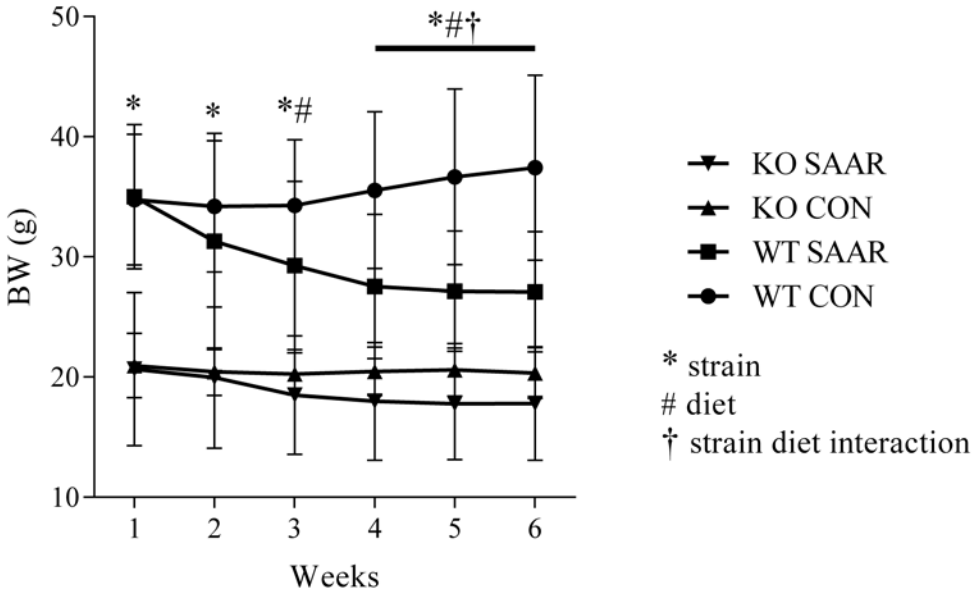

Figure 1. Change in BW. 6-8 week old WT and *Atf4* KO mice were acclimated 1 week to CON (60% fat by kcal, 20% protein, 0% cysteine, .86% methionine). Mice were either maintained on CON or randomly assigned to SAAR (60% fat by kcal, 20% protein, 0% cysteine, .12% methionine) for 5 weeks. SAAR reduces BW in WT mice. In WT CON, WT SAAR, KO CON and KO SAAR n= 3, 7, 4, 7 for females and 4, 11, 3, 5 for males.

Two-way ANOVA was performed on average BW for each week. Week 1: Effect of strain $F(1, 40)=31.178$, $p=.00000$. Week 2: Effect of strain $F(1, 40)=29.312$, $p=.00000$. Week 3: Effect of strain $F(1, 41)=42.099$, $p=.00000$, and diet $F(1, 41)=3.9582$, $p=.05334$. Week 4: Effect of strain $F(1, 41)=48.808$, $p=.00000$; diet $F(1, 41)=9.5775$, $p=.00354$; strain-diet $F(1, 41)=2.8519$, $p=.09886$. Week 5: Effect of strain $F(1, 41)=59.441$, $p=.0000$; diet $F(1, 41)=15.056$, $p=.00037$; strain-diet $F(1, 41)=4.7918$, $p=.03435$, Tukey HSD WT CON > WT SAAR, KO CON and KO SAAR $p=0.000631$, $p=0.000163$ and $p=0.000162$. WT SAAR> KO CON and KO SAAR $p=0.031328$ and $p=0.000298$. Week 6: Effect of strain $F(1, 41)=63.517$, $p=.00000$; diet $F(1, 41)=16.300$, $p=.00023$; strain-diet $F(1, 41)=6.3470$, $p=.01575$, Tukey HSD WT CON > WT SAAR, KO CON, KO SAAR, $p=0.000312$, $p=0.000162$ and $p=0.000162$. WT SAAR > KO CON and KO SAAR $p=0.025885$ and $p=0.000328$). Means are presented ± SD.

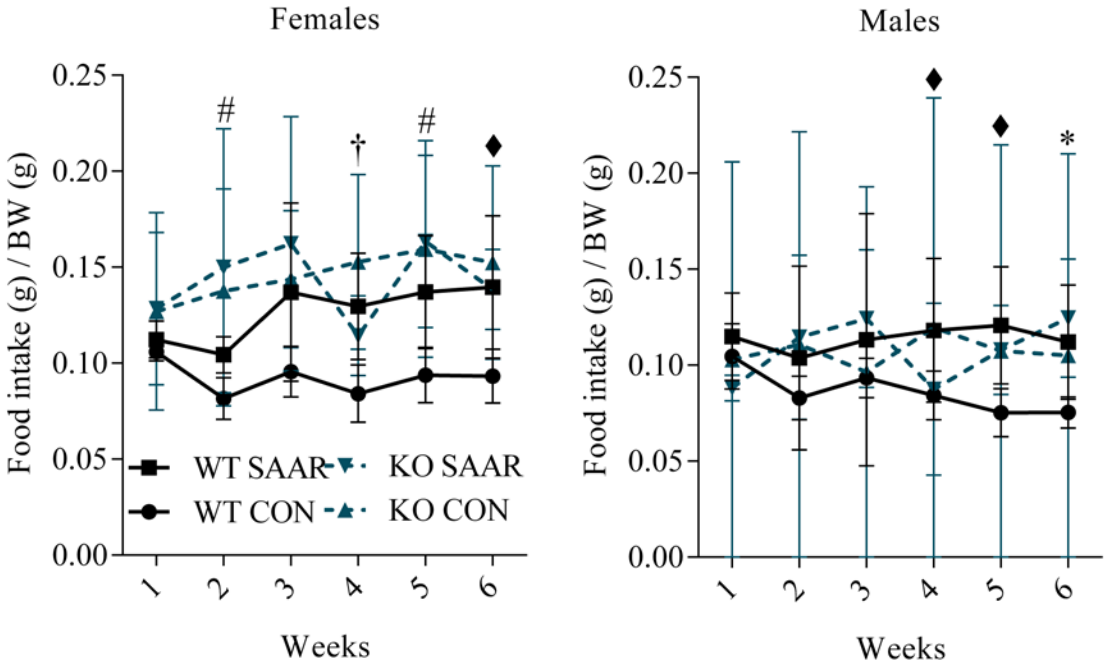

Figure 2. Weekly average of daily food intake per gram of bodyweight. 6-8 week old WT and *Atf4* KO mice were acclimated 1 week to CON (60% fat by kcal, 20% protein, 0% cysteine, .86% methionine). Mice were either maintained on CON or randomly assigned to SAAR (60% fat by kcal, 20% protein, 0% cysteine, .12% methionine) for 5 weeks. SAAR does not require ATF4 to increase food intake in males. In WT CON, WT SAAR, KO CON and KO SAAR n= 3, 7, 5, 7 for females and 4, 11, 3, 5 for males.

Two-way ANOVA was performed at each week for each sex. For females, week 2 effect of strain $F(1, 18)=4.4109$, $p=.05007$; week 4 effect of strain $F(1, 18)=3.2138$, $p=.08984$, strain-diet interaction $F(1, 18)=7.9594$, $p=.01131$, Tukey HSD KO CON > WT CON $p=0.046944$; week 5 effect of strain $F(1, 18)=5.0751$, $p=.03699$; week 6 effect of strain $F(1, 18)=3.5129$, $p=.07722$, and strain-diet $F(1, 18)=3.5348$, $p=.07638$ Tukey HSD ns. For males, there was an effect of diet at week 4 $F(1, 19)=3.4533$, $p=.07869$; week 5 $F(1, 19)=3.1237$, $p=.09322$; and week 6 $F(1, 19)=4.4575$, $p=.04822$.

* denotes effect of diet $p<.05$. # denotes effect of strain $p<.05$. † denotes strain-diet interaction $p<.05$. ♦denotes trending effect $p<.1$. Means are presented ± SD.

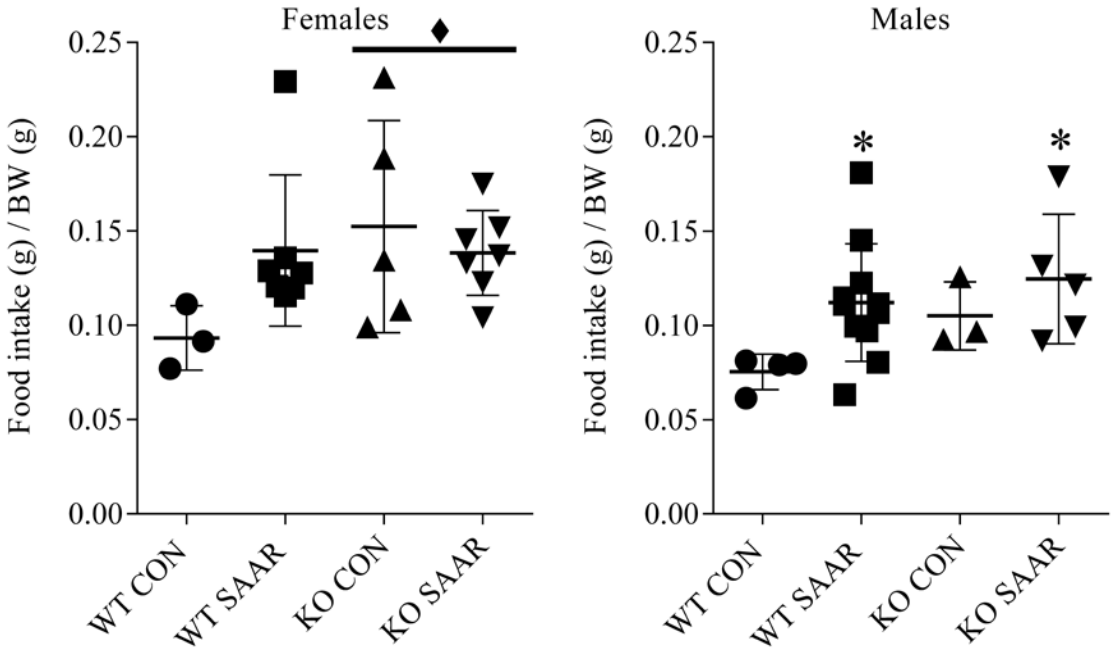

Figure 3. Average daily food intake per gram of bodyweight after 5 weeks of treatment. 6-8 week old WT and *Atf4* KO mice were acclimated 1 week to CON (60% fat by kcal, 20% protein, 0% cysteine, .86% methionine). Mice were either maintained on CON or randomly assigned to SAAR (60% fat by kcal, 20% protein, 0% cysteine, .12% methionine) for 5 weeks. SAAR does not require ATF4 to increase food intake in males. In WT CON, WT SAAR, KO CON and KO SAAR n= 3, 7, 5, 7 for females and 4, 11, 3, 5 for males.

Multifactorial ANOVA performed on combined male and female data with sex, strain and diet as factors found an effect of strain $F(1, 37)=6.0153$, $p=.01902$ and sex $F(1, 37)=6.5367$, $p=.01480$ with trending effect of diet $F(1, 37)=3.7966$, $p=.05897$ and trending strain-diet interaction $F(1, 37)=3.5167$, $p=.06866$, Tukey HSD KO CON and KO SAAR > WT CON $p= 0.015525$ and $p=0.015725$.

Two-way ANOVA performed on female data found a trending effect of strain $F(1, 18)=3.5129$, $p=.07722$ and trending strain-diet interaction $F(1, 18)=3.5348$, $p=.07638$, Tukey HSD ns. Two-way ANOVA performed on male data found an effect of diet $F(1, 19)=4.4575$, $p=.04822$. Graphs are annotated to reflect the results of individual two-way ANOVA. * denotes main effect of diet $p<.05$, and ♦ denotes trending effect $p<.1$. Means are presented ± SD.

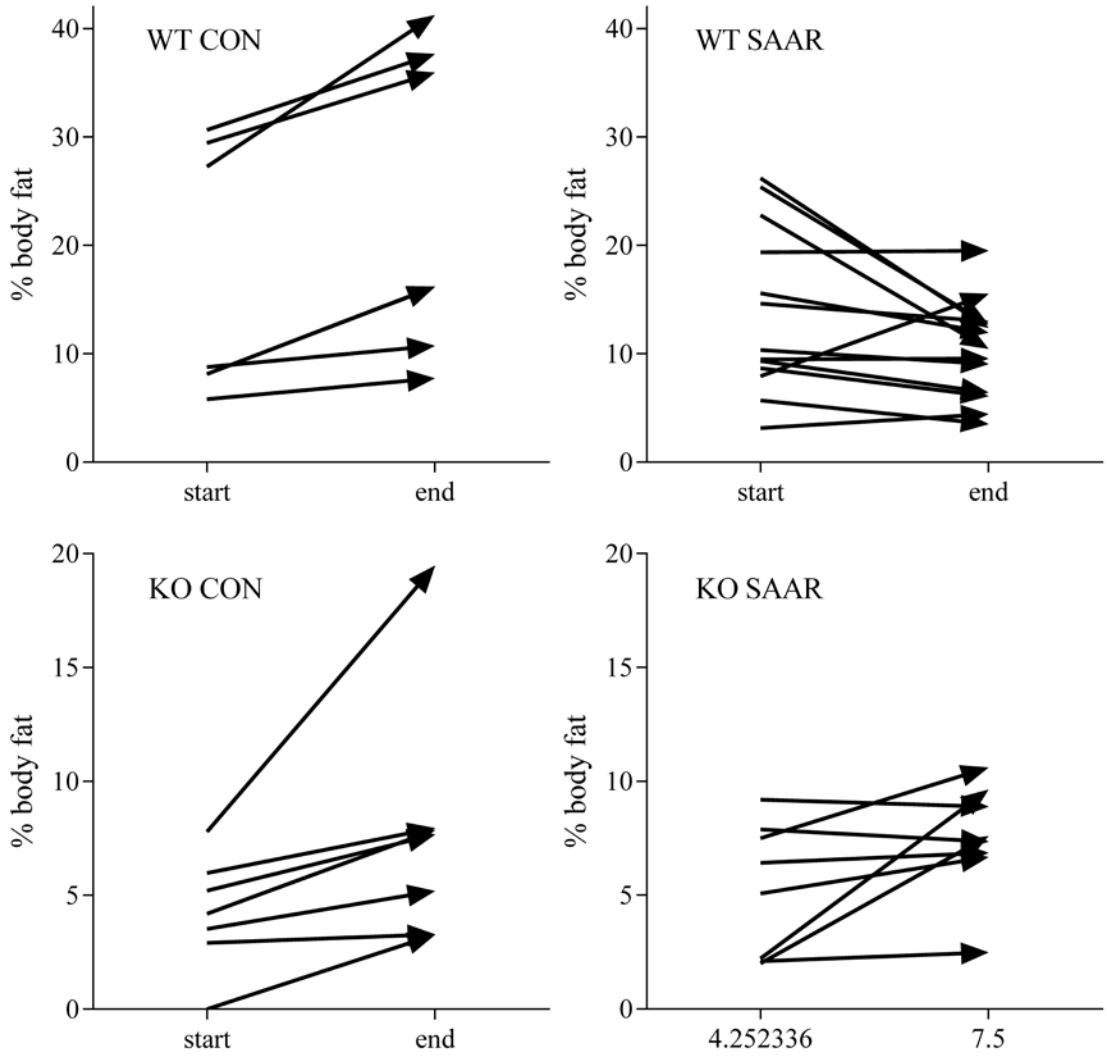

Figure 4. Initial and final percent body fat. 6-8 week old WT and *Atf4* KO mice were acclimated 1 week to CON (60% fat by kcal, 20% protein, 0% cysteine, .86% methionine). Mice were either maintained on CON or randomly assigned to SAAR (60% fat by kcal, 20% protein, 0% cysteine, .12% methionine) for 5 weeks. SAAR requires ATF4 to prevent increased adiposity. Due to increased variation when mice of SW and C57 backgrounds are combined, the small number of C57s in WT SAAR and KO SAAR were excluded from this analysis. In WT CON, WT SAAR, KO CON and KO SAAR n= 3, 4, 4, 4 for females and 4, 9, 3, 5 for males. One paired two-tailed T-Test was performed for each treatment group. Percent body fat increased significantly in WT CON, KO CON and KO SAAR p=.004762, p=.043675 and p=.035242. Means, standard deviations, t statistics and degrees of freedom can be found in Table 4.

	Mean	Std.Dv.	N	Diff.	Std.Dv. - Diff.	t	df	p
WT CON end	23.66679	14.06524						
WT CON start	16.88732	11.52062	7	6.77947	4.112452	4.36158	6	0.004762
WT SAAR end	10.35064	4.539613						
WT SAAR start	13.73418	7.600321	13	-3.38355	6.132920	-1.98919	12	0.069968
KO CON end	7.819034	5.537400						
KO CON start	4.229352	2.478643	7	3.58968	3.729075	2.54685	6	0.043675
KO SAAR end	7.509455	2.300179						
KO SAAR start	5.181448	2.729456	9	2.32801	2.760209	2.53025	8	0.035242

Table 1. Statistical output for paired two-tailed T-Tests associated with Figure 4, initial and final percent body fat. 6-8 week old WT and *Atf4* KO mice were acclimated 1 week to CON (60% fat by kcal, 20% protein, 0% cysteine, .86% methionine). Mice were either maintained on CON or randomly assigned to SAAR (60% fat by kcal, 20% protein, 0% cysteine, .12% methionine) for 5 weeks. Due to increased variation when mice of SW and C57 backgrounds were combined, the small number of C57s in WT SAAR and KO SAAR were excluded from this analysis. In WT CON, WT SAAR, KO CON and KO SAAR n= 3, 4, 4, 4 for females and 4, 9, 3, 5 for males. One paired two-tailed T-Test was performed for each treatment group. Percent body fat increased significantly in WT CON, KO CON and KO SAAR p=.004762, p=.043675 and p=.035242.

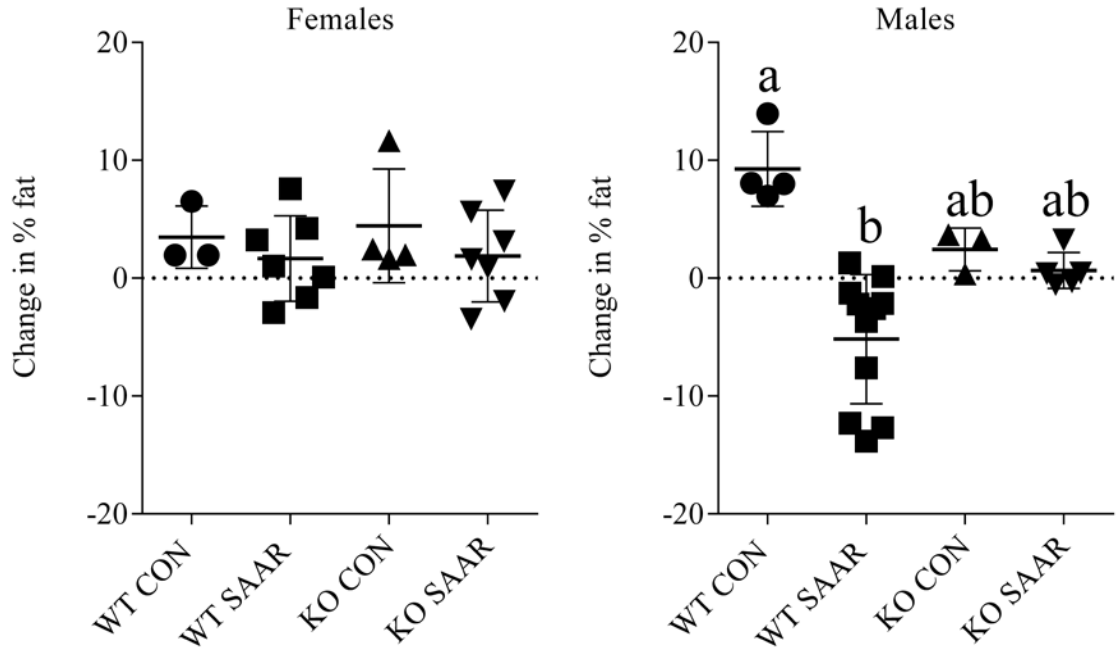

Figure 5. Change in percent body fat, calculated as % body fat after the fifth week of treatment - % body fat after 1 week acclimation to CON. 6-8 week old WT and *Atf4* KO mice were acclimated 1 week to CON (60% fat by kcal, 20% protein, 0% cysteine, .86% methionine). Mice were either maintained on CON or randomly assigned to SAAR (60% fat by kcal, 20% protein, 0% cysteine, .12% methionine) for 5 weeks. SAAR improves body composition in males but not females. In WT CON, WT SAAR, KO CON and KO SAAR n= 3, 7, 4, 7 for females and 4, 11, 3, 5 for males.

Multifactorial ANOVA was performed on combined male and female data with sex, strain and diet as factors. There was an effect of diet $F(1, 36)=14.624$, $p=.00050$, strain-diet $F(1, 36)=4.8604$, $p=.03396$, diet-sex $F(1, 36)=4.8287$, $p=.03451$. There was also strain-diet-sex interaction $F(1, 36)=6.1687$, $p=.01779$. Tukey HSD Male WT SAAR < Male WT CON, Female WT CON, Female WT SAAR, Female KO CON, Female KO SAAR $p=0.000142$, $p=0.045941$, $p=0.027516$, $p=0.006032$, and $p=0.020662$. Each graph is annotated only to reflect effects of strain and diet.

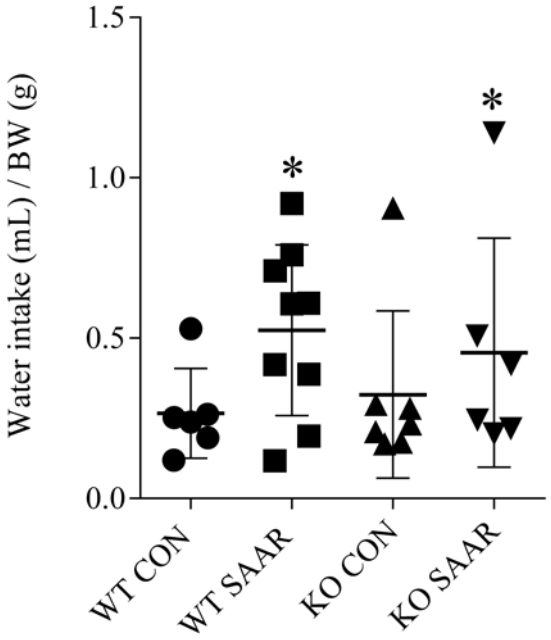

Figure 6. 48 hour cumulative water intake per gram of bodyweight after 5 weeks treatment. 6-8 week old WT and *Atf4* KO mice were acclimated 1 week to CON (60% fat by kcal, 20% protein, 0% cysteine, .86% methionine). Mice were either maintained on CON or randomly assigned to SAAR (60% fat by kcal, 20% protein, 0% cysteine, .12% methionine) for 5 weeks. SAAR does not require ATF4 to increase water intake. Males and females were combined. WT CON, WT SAAR, KO CON and KO SAAR, n= 2, 3, 5, 5 for females and 4, 6, 2, 1 for males.

Water intake (mL) was log-transformed to meet assumptions of normality, and two-way ANOVA was performed on log-transformed water intake (mL) / BW (g) with strain and diet as factors. Effect of diet $F(1, 24)=5.9231$, $p=.02276$. * denotes main effect of diet $p<.05$. Means are presented ± SD.

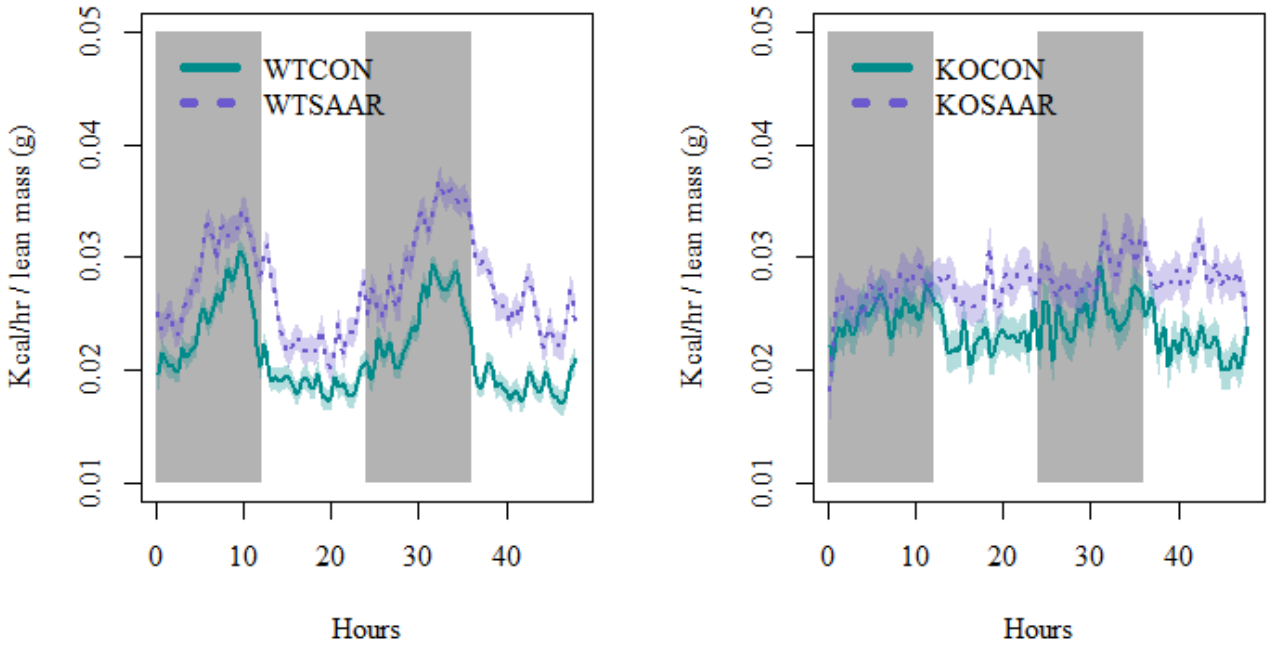

Figure 7. Diurnal rhythms in energy expenditure of male mice. 6-8 week old WT and *Atf4* KO mice were acclimated 1 week to CON (60% fat by kcal, 20% protein, 0% cysteine, .86% methionine). Mice were either maintained on CON or randomly assigned to SAAR (60% fat by kcal, 20% protein, 0% cysteine, .12% methionine) for 5 weeks. In WT CON, WT SAAR, KO CON and KO SAAR n= 8, 11, 5, 5. Group averages are graphed with 95% CI shaded behind them. Gray bars represent dark periods.

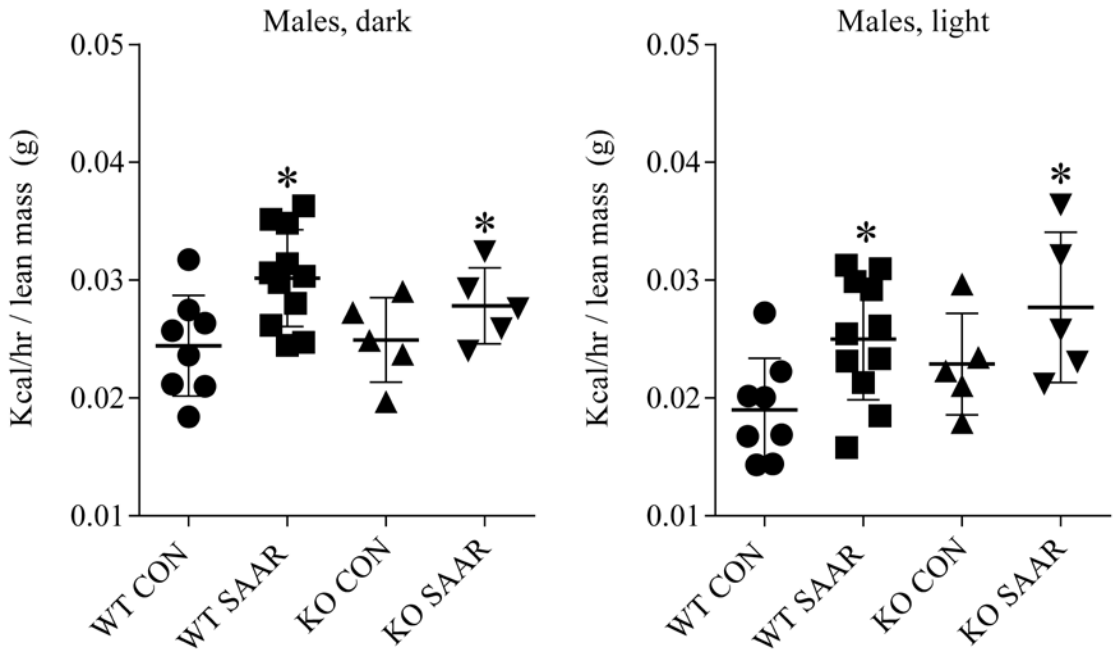

Figure 8. Average kcal/hr per gram of lean mass after 5 weeks treatment. 6-8 week old WT and *Atf4* KO mice were acclimated 1 week to CON (60% fat by kcal, 20% protein, 0% cysteine, .86% methionine). Mice were either maintained on CON or randomly assigned to SAAR (60% fat by kcal, 20% protein, 0% cysteine, .12% methionine) for 5 weeks. SAAR does not require ATF4 to increase energy expenditure in males. In WT CON, WT SAAR, KO CON and KO SAAR n= 8, 11, 5, 5 for males. ANCOVA was performed on combined light and dark data (Kcal/hr) with lean mass (g) as a covariate and period, strain and diet as factors. Effect of diet $F(1, 49)=15.180$, $p=.00030$. Effect of period $F(1, 49)=6.9794$, $p=.01104$. Trending strain-period interaction $F(1, 49)=3.2747$, $p=.07649$, Tukey HSD WT dark > WT light, KO dark and KO light $p=0.002518$, $p=0.000215$, and $p=0.000171$. * denotes effect of diet $p<.05$. Means are presented ± SD.

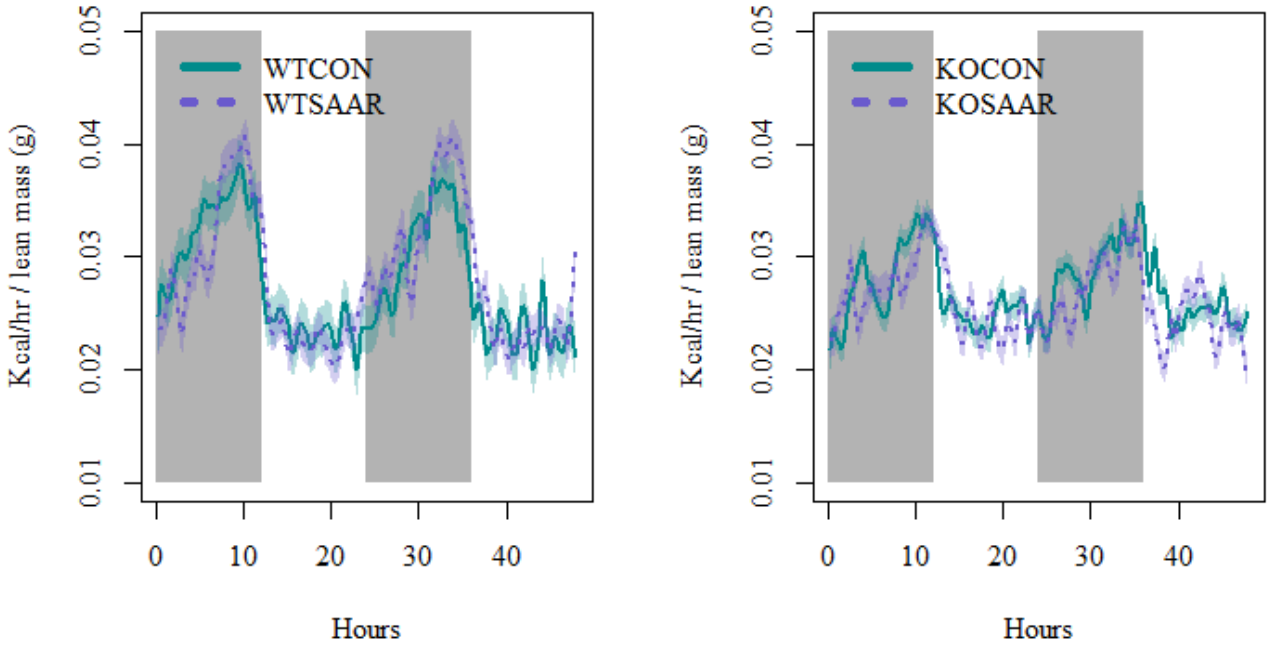

Figure 9. Diurnal rhythms in energy expenditure of female mice. 6-8 week old WT and *Atf4* KO mice were acclimated 1 week to CON (60% fat by kcal, 20% protein, 0% cysteine, .86% methionine). Mice were either maintained on CON or randomly assigned to SAAR (60% fat by kcal, 20% protein, 0% cysteine, .12% methionine) for 5 weeks. In WT CON, WT SAAR, KO CON and KO SAAR n= 5,5,7,7. Group averages are graphed with 95% CI shaded behind them. Gray bars represent dark periods.

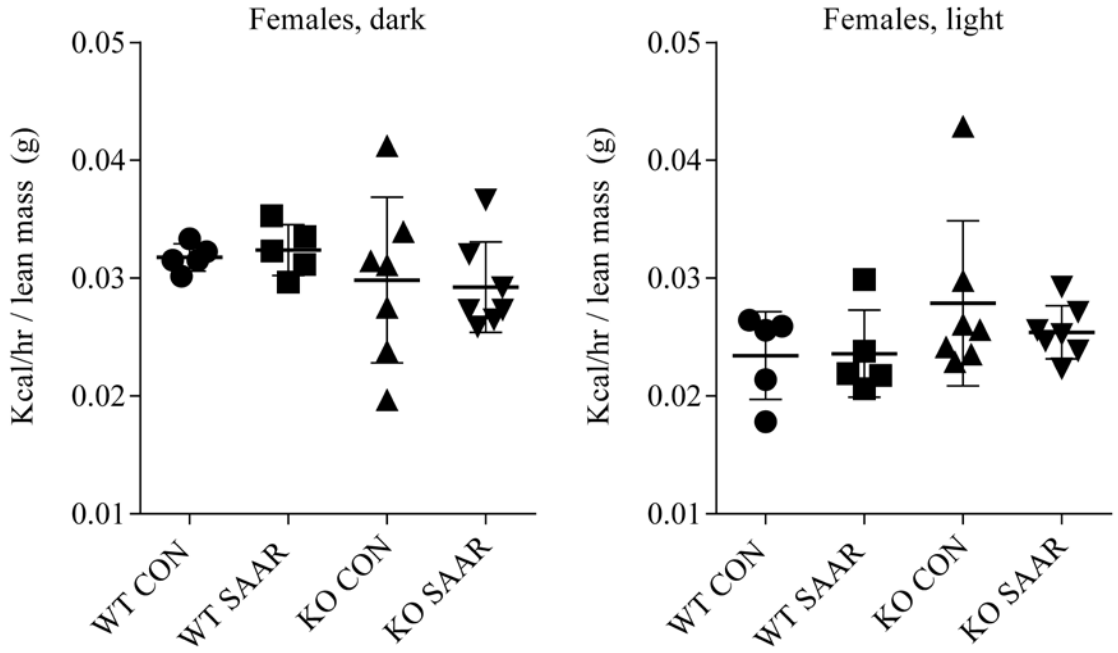

Figure 10. Average kcal/hr per gram of lean mass during the final week of a 5-week treatment period. 6-8 week old WT and *Atf4* KO mice were acclimated 1 week to CON (60% fat by kcal, 20% protein, 0% cysteine, .86% methionine). Mice were either maintained on CON or randomly assigned to SAAR (60% fat by kcal, 20% protein, 0% cysteine, .12% methionine) for 5 weeks. SAAR does not alter energy expenditure in females. In WT CON, WT SAAR, KO CON and KO SAAR n= 5, 5, 7, 7 for females. ANCOVA was performed on combined light and dark data (Kcal/hr) with lean mass (g) as a covariate and period, strain and diet as factors. There was a significant effect of period $F(1, 39)=18.097$, $p=.00013$ and an interaction between strain and period $F(1, 39)=6.7748$, $p=.01301$, Tukey HSD WT dark > WT light, KO dark and KO light $p=0.000484$, $p=0.000168$ and $p=0.000164$. Means are presented ± SD.

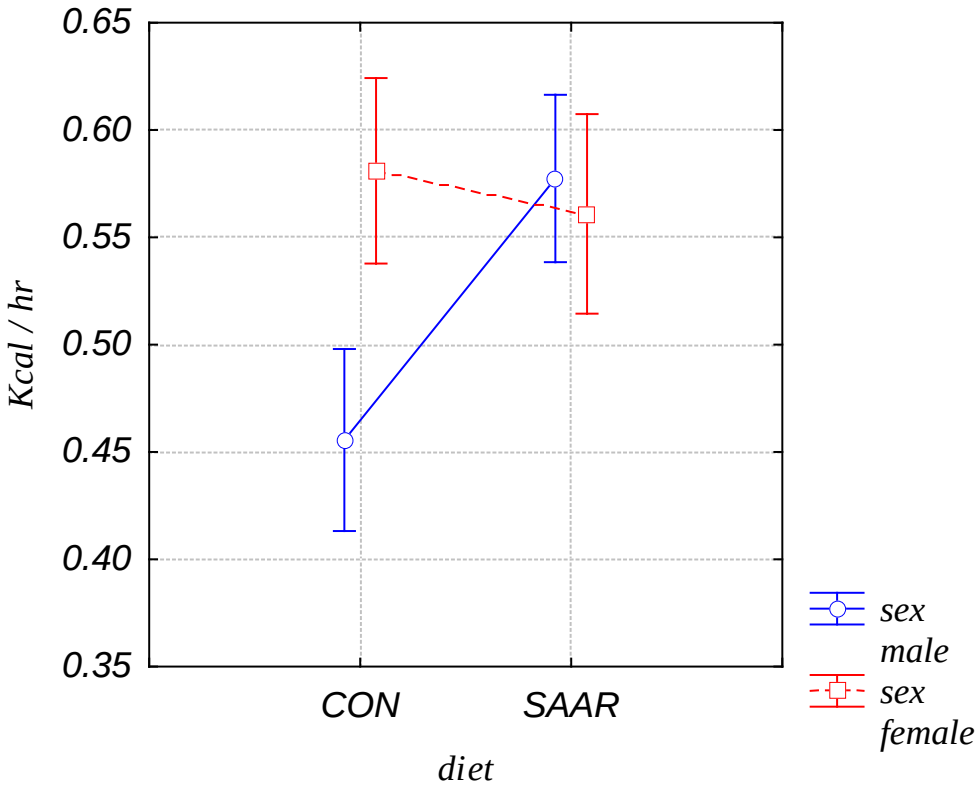

Figure 11. Sex-diet interaction seen in energy expenditure (kcal/hr) adjusted for lean mass (g) after 5 weeks treatment. 6-8 week old WT and *Atf4* KO mice were acclimated 1 week to CON (60% fat by kcal, 20% protein, 0% cysteine, .86% methionine). Mice were either maintained on CON or randomly assigned to SAAR (60% fat by kcal, 20% protein, 0% cysteine, .12% methionine) for 5 weeks. SAAR does not alter energy expenditure in females. In WT CON, WT SAAR, KO CON and KO SAAR n= 5, 5, 7, 7 for females and 8, 11, 5, 5 for males.

ANCOVA was performed on combined male and female, light and dark period data (Kcal/hr) with lean mass (g) as a covariate and sex, period, strain and diet as factors. There were significant effects of sex $F(1, 89)=4.9805$, $p=.02815$, period $F(1, 89)=20.816$, $p=.00002$ and diet $F(1, 89)=6.0672$, $p=.01570$ and strain-period interaction ($F(1, 89)=8.5960$, $p=.00428$). For the sex-diet interaction shown here $F(1, 89)=12.136$, $p=.00077$ and Tukey HSD Male SAAR > Male CON, Female SAAR and Female CON $p=0.000329$, $p=0.000144$ and $p=0.000272$. Kcal/hr is computed for covariates at their means. Vertical bars denote 95% confidence intervals.

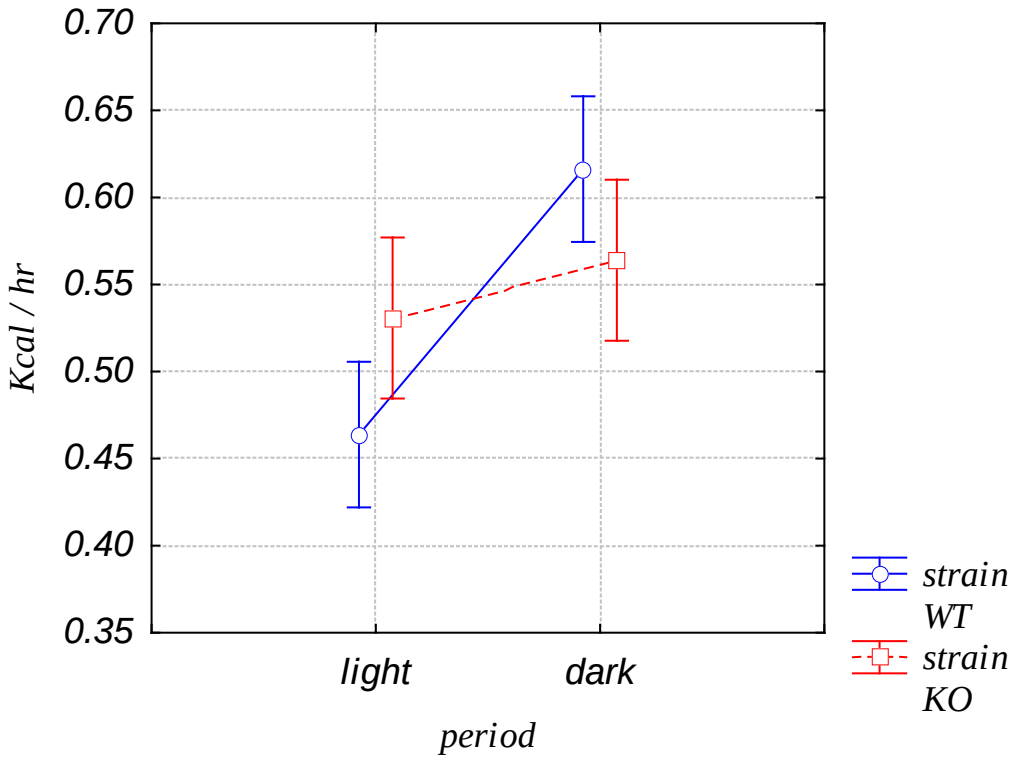

Figure 12. Strain-period interaction seen in energy expenditure (kcal/hr) adjusted for lean mass (g), after 5 weeks treatment. 6-8 week old WT and Atf4 KO mice were acclimated 1 week to CON (60% fat by kcal, 20% protein, 0% cysteine, .86% methionine). Mice were either maintained on CON or randomly assigned to SAAR (60% fat by kcal, 20% protein, 0% cysteine, .12% methionine) for 5 weeks. *Atf4* KO reduces diurnal fluctuation in energy expenditure. In WT CON, WT SAAR, KO CON and KO SAAR n= 5, 5, 7, 7 for females and 8, 11, 5, 5 for males.

ANCOVA was performed on combined male and female, light and dark period data (Kcal/hr) with lean mass (g) as a covariate and sex, period, strain and diet as factors. There were significant effects of sex $F(1, 89)=4.9805$, $p=.02815$, period $F(1, 89)=20.816$, $p=.00002$ and diet $F(1, 89)=6.0672$, $p=.01570$ and sex-diet interaction $F(1, 89)=12.136$, $p=.00077$. For the strain-period interaction shown here ($F(1, 89)=8.5960$, $p=.00428$) and Tukey HSD WT dark > WT light, KO dark, and KO light $p= 0.000146$, $p=0.000144$, and $p= 0.000144$. KO light > WT light $p= 0.001387$. Kcal/hr is computed for covariates at their means. Vertical bars denote 95% confidence intervals.

	Females				*Males*			
÷ BW	WT CON	WT SAAR	KO CON	KO SAAR	WT CON	WT SAAR	KO CON	WT CON
Liver	0.015 ± 0.016	0.030 ± 0.011	0.013 ± 0.013	0.035 ± 0.011	0.036 ± 0.030	0.033 ± 0.010	0.027 ± 0.007	0.031 ± 0.004
Gon Fat	0.052 ± 0.032 **a**	0.021 ± 0.007 **b**	0.019 ± 0.008 **b**	0.008 ± 0.004 **b**	0.107 ± 0.070 **a**	0.027 ± 0.010 **b**	0.010 ± 0.007 **b**	0.012 ± 0.004 **b**
Sub Q fat	0.028 ± 0.011 **ab**	0.016 ± 0.006 **b**	0.016 ± 0.002 **ab**	0.009 ± 0.004 **b**	0.053 ± 0.044 **a**	0.012 ± 0.005 **b**	0.009 ± 0.002 **b**	0.010 ± 0.004 **b**
Heart	0.006 ± 0.001	0.006 ± 0.001	0.007 ± 0.002	0.006 ± 0.002	0.007 ± 0.003	0.006 ± 0.001	0.006 ± 0.001	0.007 ± 0.001
Gastroc	0.009 ± 0.001	0.011 ± 0.002	0.011 ± 0.002	0.011 ± 0.002	0.011 ± 0.005	0.011 ± 0.002	0.010 ± 0.001	0.011 ± 0.001
Soleus	0.001 ± 0.000	0.001 ± 0.000	0.001 ± 0.000	0.002 ± 0.002	0.001 ± 0.000	0.001 ± 0.001	0.001 ± 0.000	0.001 ± 0.000
Kidney	0.012 ± 0.001	0.013 ± 0.001	0.016 ± 0.002	0.012 ± 0.003	0.014 ± 0.006	0.014 ± 0.002	0.015 ± 0.001	0.014 ± 0.001
Spleen	0.004 ± 0.000	0.003 ± 0.001	0.004 ± 0.000	0.003 ± 0.001	0.003 ± 0.002	0.003 ± 0.001	0.003 ± 0.000	0.007 ± 0.010
Brain	0.015 ± 0.002 **a**	0.016 ± 0.007 **a**	0.019 ± 0.002 **b**	0.023 ± 0.006 **b**	0.014 ± 0.005 **a**	0.015 ± 0.005 **a**	0.017 ± 0.002 **b**	0.017 ± 0.002 **b**

Table 2. Tissue weights after five weeks of treatment. 6-8 week old WT and *Atf4* KO mice were acclimated 1 week to CON (60% fat by kcal, 20% protein, 0% cysteine, .86% methionine). Mice were either maintained on CON or randomly assigned to SAAR (60% fat by kcal, 20% protein, 0% cysteine, .12% methionine) for 5 weeks. In WT CON, WT SAAR, KO CON and KO SAAR n= 3, 7, 3, 7 for females and 4, 11, 3, 5 for males.

In gonadal fat, there was a significant effect of strain ($F(1, 35)=19.225$, $p=.00010$), diet ($F(1, 35)=10.929$, $p=.00219$) and strain-diet ($F(1, 35)=7.9508$, $p=.00786$, Tukey HSD WT CON > WT SAAR, KO CON, KO SAAR $p= 0.000263$, $p= 0.000402$, $p= 0.000165$). In subcutaneous fat there was an effect of strain ($F(1, 35)=9.4051$, $p=.00416$), diet ($F(1, 35)=7.4864$, $p=.00970$), strain-diet ($F(1, 35)=4.6589$, $p=.03783$, Tukey HSD) and sex-strain-diet ($F(1, 35)=3.0811$, $p=.08796$, Tukey HSD Male WT CON > Male WT SAAR, Male KO CON, Male KO SAAR, Female WT SAAR, Female KO SAAR $p= 0.002146$, $p= 0.015586$, $p= 0.005032$, $p= 0.012485$, $p= 0.001886$). In brain there was an effect of strain ($F(1, 35)=5.4082$, $p=.02596$).

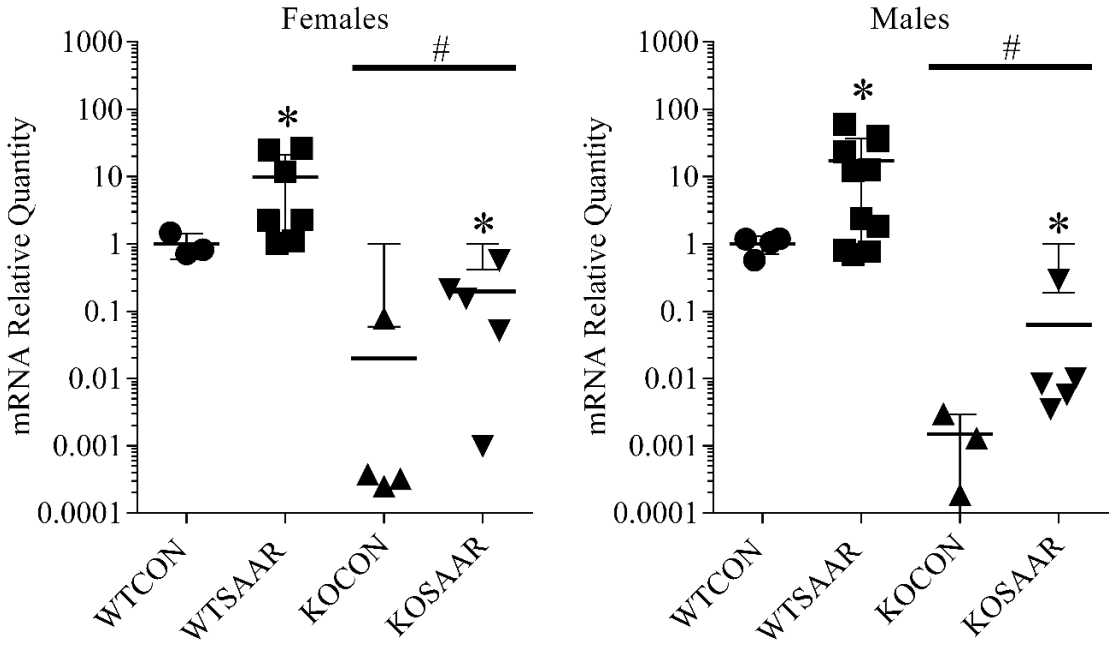

Figure 13. Hepatic *Atf4* expression after 5 weeks of treatment. 6-8 week old WT and *Atf4* KO mice were acclimated 1 week to CON (60% fat by kcal, 20% protein, 0% cysteine, .86% methionine). Mice were either maintained on CON or randomly assigned to SAAR (60% fat by kcal, 20% protein, 0% cysteine, .12% methionine) for 5 weeks. SAAR increases hepatic *Atf4*. In WT CON, WT SAAR, KO CON and KO SAAR n= 3, 7, 4, 7 for females and 4, 11, 3, 5 for males. Multifactorial ANOVA was performed on log transformed, combined male and female data with sex, strain and diet as factors. Effect of strain $F(1, 35)=53.831$, $p=.00000$. Effect of diet $F(1, 35)=7.3004$, $p=.01056$. * denotes main effect of diet $p<.05$, and # denotes main effect of strain $p<.05$. Means are presented ± SD.

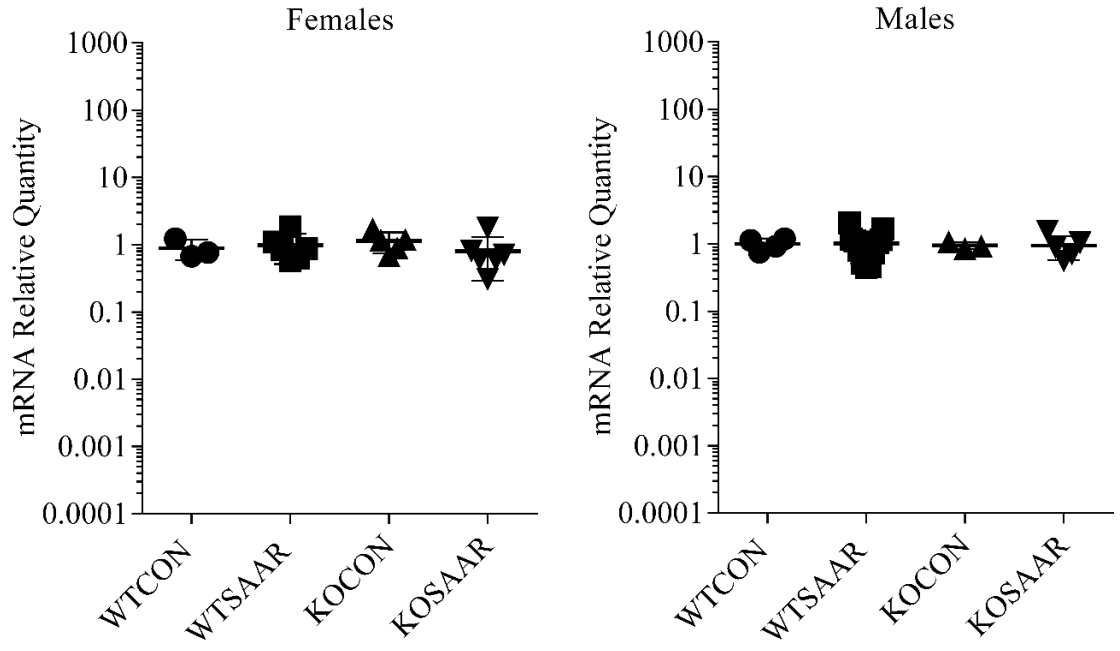

Figure 14. Hepatic *Atf5* expression after 5 weeks of treatment. 6-8 week old WT and *Atf4* KO mice were acclimated 1 week to CON (60% fat by kcal, 20% protein, 0% cysteine, .86% methionine). Mice were either maintained on CON or randomly assigned to SAAR (60% fat by kcal, 20% protein, 0% cysteine, .12% methionine) for 5 weeks. SAAR does not alter hepatic *Atf5*. In WT CON, WT SAAR, KO CON and KO SAAR n= 3, 7, 5, 7 for females and 4, 11, 3, 5 for males. Multifactorial ANOVA was performed on log transformed, combined male and female data with sex, strain and diet as factors. Means are presented ± SD.

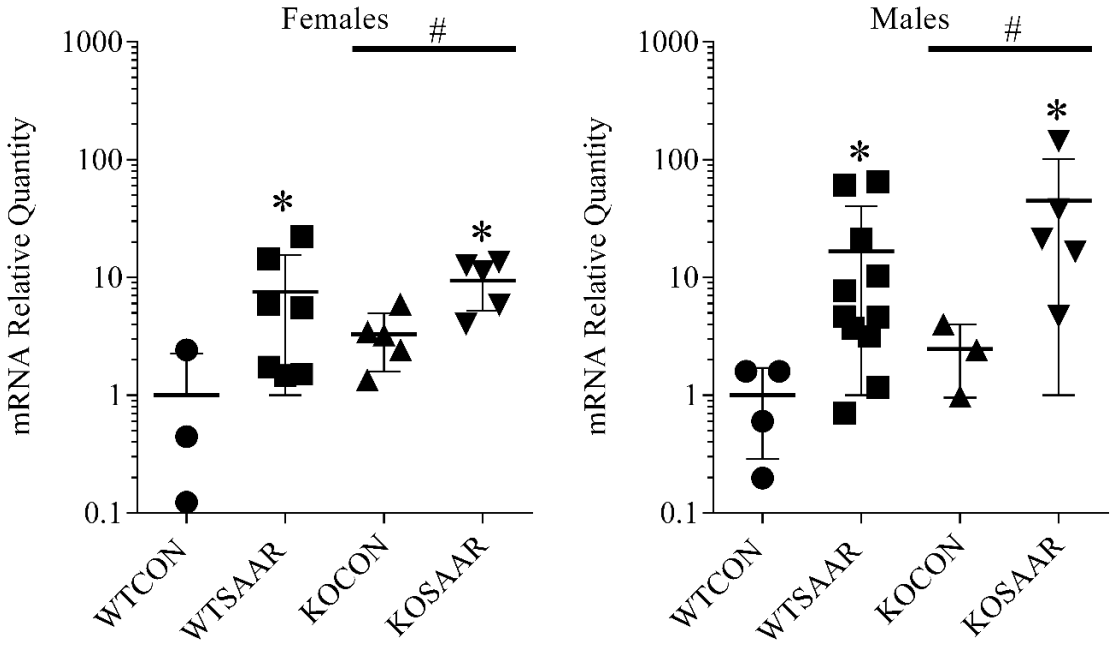

Figure 15. Hepatic *Fgf21* expression after 5 weeks of treatment. 6-8 week old WT and *Atf4* KO mice were acclimated 1 week to CON (60% fat by kcal, 20% protein, 0% cysteine, .86% methionine). Mice were either maintained on CON or randomly assigned to SAAR (60% fat by kcal, 20% protein, 0% cysteine, .12% methionine) for 5 weeks. SAAR does not require ATF4 to increase hepatic *Fgf21*. In WT CON, WT SAAR, KO CON and KO SAAR n= 3, 7, 5, 5 for females and 4, 11, 3, 5 for males. Multifactorial ANOVA was performed on log transformed, combined male and female data with sex, strain and diet as factors. Effect of strain $F(1, 36)=5.9580$, $p=.01970$. Effect of diet $F(1, 36)=18.971$, $p=.00011$. * denotes effect of diet $p<.05$. # denotes effect of strain $p<.05$. Means are presented ± SD.

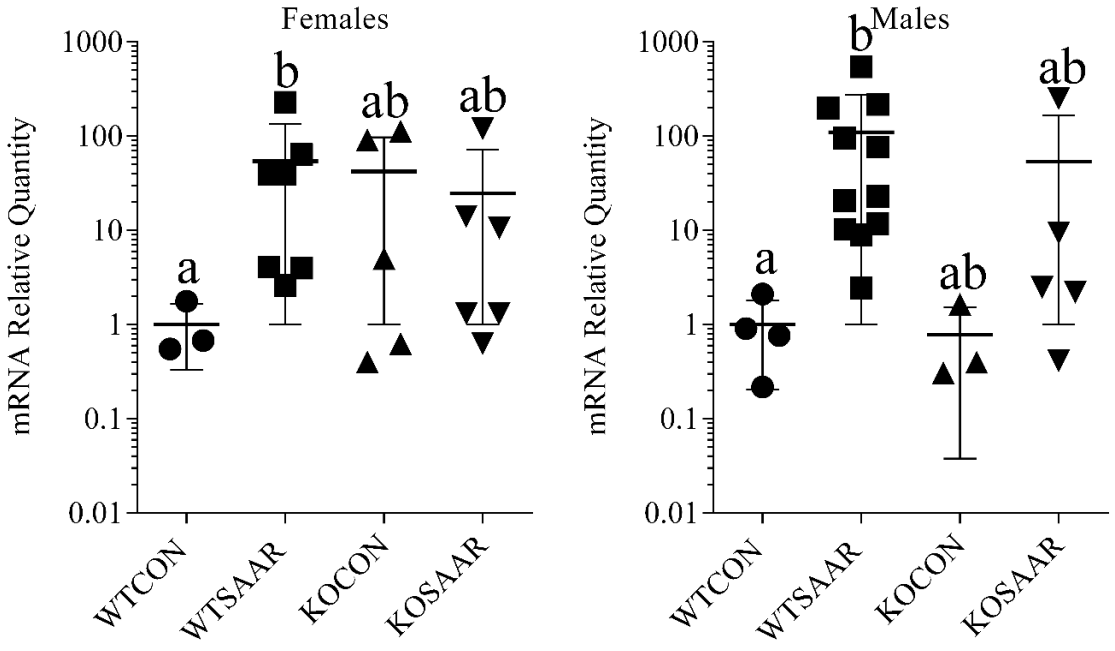

Figure 16. Hepatic *Nupr1* expression after 5 weeks of treatment. 6-8 week old WT and *Atf4* KO mice were acclimated 1 week to CON (60% fat by kcal, 20% protein, 0% cysteine, .86% methionine). Mice were either maintained on CON or randomly assigned to SAAR (60% fat by kcal, 20% protein, 0% cysteine, .12% methionine) for 5 weeks. SAAR requires ATF4 to increase hepatic *Nupr1*. In WT CON, WT SAAR, KO CON and KO SAAR n= 3, 7, 5, 6 for females and 4, 11, 3, 5 for males. Multifactorial ANOVA was performed on log transformed, combined male and female data with sex, strain and diet as factors. Effect of sex $F(1, 36)=7.9681$, $p=.00771$, Tukey HSD Females > Males $p= 0.047794$. Effect of diet $F(1, 36)=14.047$, $p=.00062$. Strain-diet interaction $F(1, 36)=4.3402$, $p=.04438$, Tukey HSD WT SAAR >WT CON $p=0.000758$. Groups without a common letter differ. Means are presented ± SD.

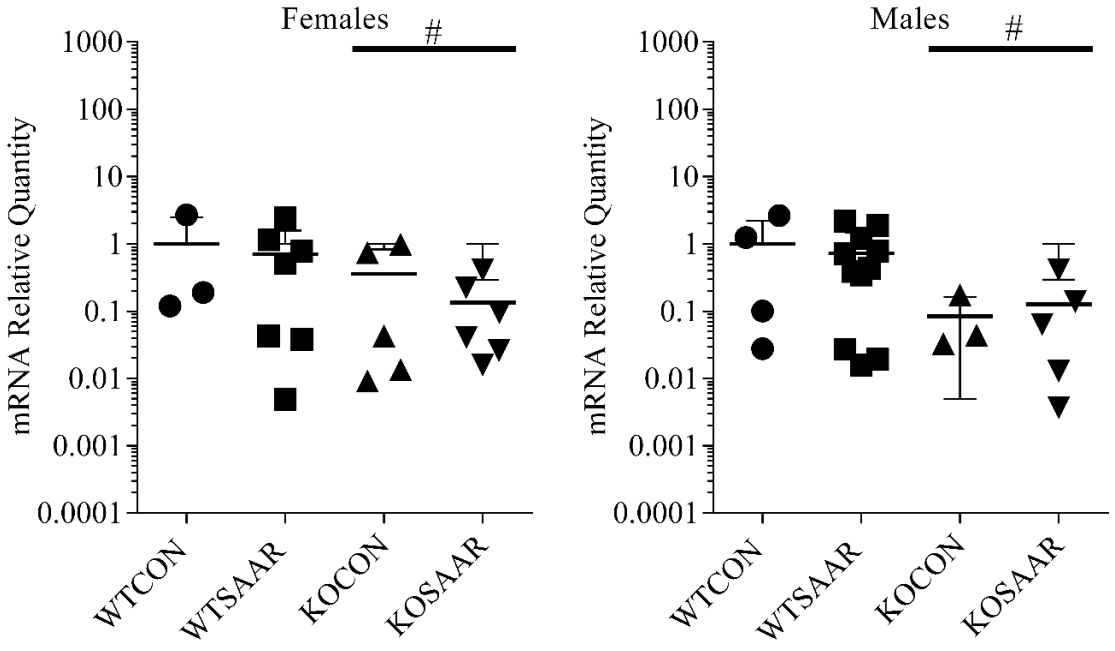

Figure 17. Hepatic *Scd1* expression after 5 weeks of treatment. 6-8 week old WT and *Atf4* KO mice were acclimated 1 week to CON (60% fat by kcal, 20% protein, 0% cysteine, .86% methionine). Mice were either maintained on CON or randomly assigned to SAAR (60% fat by kcal, 20% protein, 0% cysteine, .12% methionine) for 5 weeks. SAAR does not alter hepatic *Scd1*. In WT CON, WT SAAR, KO CON and KO SAAR n= 3, 7, 5, 6 for females and 4, 11, 3, 5 for males. Multifactorial ANOVA was performed on log transformed, combined male and female data with sex, strain and diet as factors. Effect of strain $F(1, 36)=5.9597$, $p=.01968$. # denotes effect of strain $p<.05$. Means are presented ± SD.

Discussion

The mechanisms by which loss of specific amino acids versus total protein are sensed remain unclear. The Integrated Stress Response relies on the kinase GCN2 to initiate responses to amino acid stress, yet we find GCN2 independent responses to SAAR [28] and non-overlapping responses between GCN2 and its downstream effector ATF4 during amino acid depletion induced by asparaginase [52]. To understand the role of ATF4 in altering food and water intake, energy expenditure, body composition and hepatic gene expression during SAAR, we used a model of genetic deletion of *Atf4* and a 5 week treatment period of high fat SAAR diet. We hypothesized that ATF4 would be required for a SAAR-induced whole-body phenotype of increased food and water intake, increased energy expenditure, and reduced adiposity, and that ATF4 would also be required for increased hepatic *Fgf21* expression. We expected that this whole-body phenotype would correspond with increased hepatic *Fgf21* expression, suggesting an ATF4-FGF21 axis.

In both WT and KO strains, responses to SAAR were observed, but limited to males. In context with previous work, we found ATF4 to play a complex role in the ISR: food intake is independent of both GCN2 [28] and ATF4 (Figures 2 and 3); protection from increased adiposity is GCN2-independent [28] but ATF4-dependent (Figure 4); and increased energy expenditure is GCN2-dependent [28] but ATF4-independent (Figures 7 and 8). Clearly the ISR is not best described as a simple GCN2-eIF2-ATF. Similar to asparaginase treatment [52], we find that during SAAR GCN2 and ATF4 are required separately.

That the first component of the ISR, activity of the amino-acid-sensing kinase GCN2, can be bypassed has already been seen [10], particularly in our previous study [28] where eIF2B activity was reduced in *Gcn2* KO mice despite unchanged levels of phosphorylated eIF2. An increase in phosphorylated eIF2 is the currently proposed mechanism for reduction in eIF2B activity, and a reduction in eIF2B activity should not occur otherwise. This work adds to the previous findings by showing that the next component of the ISR, ATF4 translation, can in fact be bypassed too. Our finding of elevated *Fgf21* in KO SAAR mice (Figure 15), as well as work showing *Fgf21* KO mice do not respond to SAAR [51], suggest *Fgf21* may be responsible for GCN2- and ATF4-independent responses to SAAR. It also suggests a compensatory pathway for *Fgf21* elevation in the absence of ATF4, of which there are multiple potential candidates.

Following the report of increased water intake during a protein restricted diet [78], this is the first to show water intake increased by SAAR (Figure 6). This extension of the correspondence between protein restriction and SAAR from food intake to water intake supports the application of the ISR pathway to SAAR. Although hyperphagy is accounted for by the concept of protein (or methionine) leverage, the physiological reasoning behind increased water intake remains uncertain. The protein leverage hypothesis states that food intake increases until adequate consumption of the limiting nutrient, protein, is reached. Metabolism then becomes less efficient, to offset the caloric load [4, 5]. Like hyperphagy, increased water intake may be tied to increased energy expenditure, perhaps as a thermoregulatory compensation. Or it may be coincident to increased food intake. These possibilities have yet to be tested. In agreement with findings that FGF21

administration increased water intake [78], we found that water intake closely resembled *Fgf21* expression (Figure 3), which were both significantly increased by SAAR. This suggests that SAAR increases water intake via an FGF21 axis, but via an intermediary which is not ATF4.

While we found SAAR clearly increased energy expenditure in KO mice at 5 weeks (figure 10), energy expenditure is not increased by SAAR in *Gcn2* KO [28] within the same timeframe. The GCN2-dependence but ATF4-independence of energy expenditure within this timeframe is particularly surprising because it differs from food intake, which is GCN2- and ATF4-independent. The mechanisms behind increased food intake and energy expenditure are linked theoretically according to the protein (and/or methionine) leverage hypothesis. Because these responses occur together, it is intuitive to speculate that they occur under the same control. The ISR provides a streamlined solution: one sensor-kinase leads to translation of one transcription factor, whose many targets exert many physiological effects. The way increased food intake and increased energy expenditure occur outside of (food intake) and only partially within (energy expenditure) the ISR signals the need for new conceptual frameworks.

Whether ATF4 is required for SAAR-mediated improvement in body composition is difficult to assess using this model. Global *Atf4* deletion creates a basally lean phenotype. Previous work in *Gcn2* KO mice shows a reduced increase in adiposity in KO SAAR versus KO CON [28]. However, *Gcn2* KO mice gained 15-20% body fat [28], while *Atf4*

KO mice gained less than 5 % body fat. Thus, although this study finds no difference in the increase in adiposity in KO SAAR versus KO CON, it is difficult to tell whether a difference would have been seen if KO mice were less basally lean. A more appropriate model may be liver-specific deletion of *Atf4*, as liver-specific KO mice have similar body weights and body composition to WT mice.

Although ATF4 elevates *Fgf21* during stress [49, 56, 58], we find there are redundant pathways which act to elevate hepatic *Fgf21* during SAAR when *Atf4* is globally deleted. There are several likely candidates for a compensatory pathway. Without ATF4 present, other transcription factors may be binding to the promoter of FGF21. ATF4 interacts with nuclear factor erythroid-derived 2 (Nrf2) [91], for example in regulating the expression of heme oxygenase [92]. Treatment with an *Nrf2*-inducer increases hepatic *Fgf21* expression as well as serum FGF21 in mice [93]. *Fgf21* expression is increased by peroxisome proliferator-activated receptor (PPAR) agonists in humans, specifically alpha and delta (but not gamma) [94]. PPAR-alpha regulates hepatic *Fgf21* in mice [95]. Finally, upstream of the amino acid response element (AARE) in the *Fgf21* promoter is an endoplasmic reticulum stress response element (ERSE) [91]. During ER stress, site specific splicing leads to production of X-box-binding protein 1 (XBP1) [57], which binds to the ERSE [96]. ER stress and subsequent XBP1 splicing has been shown to increase *Fgf21* expression [97]. Chromatin immunoprecipitation of the *Fgf21* promoter is necessary to identify what is binding in the absence of ATF4.

We also found that whatever mechanism increases energy expenditure during SAAR, it is likely separate from that which controls energy expenditure's diurnal rhythm, which is blunted in the absence of ATF4 (Figures 9 and 10). Diurnal rhythm in energy expenditure may normally be influenced by diurnal rhythms in *Fgf21*, which may in turn be driven by the diurnal regulation of *Atf4*. *Atf4* is regulated by the clock factor *period 2* [98], and *Fgf21* demonstrates diurnal rhythm in its expression [99]. Although *Fgf21* is elevated in the absence of ATF4 by a compensatory mechanism, it may not have the same diurnal characteristics, leading to damped fluctuations in energy expenditure. It is also possible that global *Atf4* KO reduces the diurnal rhythm of energy expenditure by disrupting feedbacks involving ATF4 in the brain [98]. Liver specific KO would be informative in determining whether the diurnal rhythm of energy expenditure is influenced directly by ATF4 in the brain. Reduced diurnal fluctuations in energy expenditure also suggest impaired metabolic flexibility. Although there was no clear disruption of RER in high fat fed KO mice (Figure 15), differences may be visible on a normal fat diet.

Overall, the ISR is more complex than a linear GCN2-eIF2-ATF4 scheme allows, and in addition to non-overlapping effects of GCN2 and ATF4 during SAAR, FGF21 is a critical mediator which should be included as an actor. Further research is necessary to clarify the effect of hepatic ATF4 during SAAR, particularly on changes in body composition. Finally, the pathway by which *Fgf21* is elevated in the absence of ATF4 must be identified.

References

1. Sanz, A., P. Caro, and G. Barja, *Protein restriction without strong caloric restriction decreases mitochondrial oxygen radical production and oxidative DNA damage in rat liver.* J Bioenerg Biomembr, 2004. **36**(6): p. 545-5210.1007/s10863-004-9001-7.
2. Jimenez Jaime, T., L. Leiva Balich, G. Barrera Acevedo, M.P. de la Maza Cave, S. Hirsch Birn, S. Henriquez Parada, J. Rodriguez Silva, and D. Bunout Barnett, *Effect of calorie restriction on energy expenditure in overweight and obese adult women.* Nutr Hosp, 2015. **31**(6): p. 2428-3610.3305/nh.2015.31.6.8782.
3. Pezeshki, A., R.C. Zapata, A. Singh, N.J. Yee, and P.K. Chelikani, *Low protein diets produce divergent effects on energy balance.* Sci Rep, 2016. **6**: p. 25145.PMC4848496. 10.1038/srep25145.
4. Simpson, S.J. and D. Raubenheimer, *Obesity: the protein leverage hypothesis.* Obes Rev, 2005. **6**(2): p. 133-4210.1111/j.1467-789X.2005.00178.x.
5. Solon-Biet, S.M., A.C. McMahon, J.W. Ballard, K. Ruohonen, L.E. Wu, V.C. Cogger, A. Warren, X. Huang, N. Pichaud, R.G. Melvin, R. Gokarn, M. Khalil, N. Turner, G.J. Cooney, D.A. Sinclair, D. Raubenheimer, D.G. Le Couteur, and S.J. Simpson, *The ratio of macronutrients, not caloric intake, dictates cardiometabolic health, aging, and longevity in ad libitum-fed mice.* Cell Metab, 2014. **19**(3): p. 418-30.PMC5087279. 10.1016/j.cmet.2014.02.009.
6. Elshorbagy, A.K., M. Valdivia-Garcia, D.A. Mattocks, J.D. Plummer, A.D. Smith, C.A. Drevon, H. Refsum, and C.E. Perrone, *Cysteine supplementation reverses methionine restriction effects on rat adiposity: significance of stearoyl-coenzyme A desaturase.* J Lipid Res, 2011. **52**(1): p. 104-12.PMC2999932. 10.1194/jlr.M010215.
7. Lees, E.K., R. Banks, C. Cook, S. Hill, N. Morrice, L. Grant, N. Mody, and M. Delibegovic, *Direct comparison of methionine restriction with leucine restriction on the metabolic health of C57BL/6J mice.* Sci Rep, 2017. **7**(1): p. 9977.PMC5577041. 10.1038/s41598-017-10381-3.
8. Wanders, D., K.P. Stone, K. Dille, J. Simon, A. Pierse, and T.W. Gettys, *Metabolic responses to dietary leucine restriction involve remodeling of adipose tissue and enhanced hepatic insulin signaling.* Biofactors, 2015. **41**(6): p. 391-402.PMC4715699. 10.1002/biof.1240.
9. Perrone, C.E., D.A. Mattocks, M. Jarvis-Morar, J.D. Plummer, and N. Orentreich, *Methionine restriction effects on mitochondrial biogenesis and aerobic capacity in white adipose tissue, liver, and skeletal muscle of F344 rats.* Metabolism, 2010. **59**(7): p. 1000-1110.1016/j.metabol.2009.10.023.
10. Laeger, T., D.C. Albarado, S.J. Burke, L. Trosclair, J.W. Hedgepeth, H.R. Berthoud, T.W. Gettys, J.J. Collier, H. Munzberg, and C.D. Morrison, *Metabolic Responses to Dietary Protein Restriction Require an Increase in FGF21 that Is Delayed by the Absence of GCN2.* Cell Rep, 2016. **16**(3): p. 707-16.PMC4956501. 10.1016/j.celrep.2016.06.044.

11. Fusakio, M.E., J.A. Willy, Y. Wang, E.T. Mirek, R.J. Al Baghdadi, C.M. Adams, T.G. Anthony, and R.C. Wek, *Transcription factor ATF4 directs basal and stress-induced gene expression in the unfolded protein response and cholesterol metabolism in the liver.* Mol Biol Cell, 2016. **27**(9): p. 1536-51.PMC4850040. 10.1091/mbc.E16-01-0039.
12. Orentreich, N., J.R. Matias, A. DeFelice, and J.A. Zimmerman, *Low methionine ingestion by rats extends life span.* J Nutr, 1993. **123**(2): p. 269-7410.1093/jn/123.2.269.
13. Sikalidis, A.K. and M.H. Stipanuk, *Growing rats respond to a sulfur amino acid-deficient diet by phosphorylation of the alpha subunit of eukaryotic initiation factor 2 heterotrimeric complex and induction of adaptive components of the integrated stress response.* J Nutr, 2010. **140**(6): p. 1080-5.PMC2869497. 10.3945/jn.109.120428.
14. Richie, J.P., Jr., Y. Leutzinger, S. Parthasarathy, V. Malloy, N. Orentreich, and J.A. Zimmerman, *Methionine restriction increases blood glutathione and longevity in F344 rats.* FASEB J, 1994. **8**(15): p. 1302-7
15. Malloy, V.L., R.A. Krajcik, S.J. Bailey, G. Hristopoulos, J.D. Plummer, and N. Orentreich, *Methionine restriction decreases visceral fat mass and preserves insulin action in aging male Fischer 344 rats independent of energy restriction.* Aging Cell, 2006. **5**(4): p. 305-1410.1111/j.1474-9726.2006.00220.x.
16. Plaisance, E.P., F.L. Greenway, A. Boudreau, K.L. Hill, W.D. Johnson, R.A. Krajcik, C.E. Perrone, N. Orentreich, W.T. Cefalu, and T.W. Gettys, *Dietary methionine restriction increases fat oxidation in obese adults with metabolic syndrome.* J Clin Endocrinol Metab, 2011. **96**(5): p. E836-40.PMC3085194. 10.1210/jc.2010-2493.
17. Elshorbagy, A.K., M. Valdivia-Garcia, H. Refsum, A.D. Smith, D.A. Mattocks, and C.E. Perrone, *Sulfur amino acids in methionine-restricted rats: hyperhomocysteinemia.* Nutrition, 2010. **26**(11-12): p. 1201-410.1016/j.nut.2009.09.017.
18. Malloy, V.L., C.E. Perrone, D.A. Mattocks, G.P. Ables, N.S. Caliendo, D.S. Orentreich, and N. Orentreich, *Methionine restriction prevents the progression of hepatic steatosis in leptin-deficient obese mice.* Metabolism, 2013. **62**(11): p. 1651-6110.1016/j.metabol.2013.06.012.
19. Pacana, T., S. Cazanave, A. Verdianelli, V. Patel, H.K. Min, F. Mirshahi, E. Quinlivan, and A.J. Sanyal, *Dysregulated Hepatic Methionine Metabolism Drives Homocysteine Elevation in Diet-Induced Nonalcoholic Fatty Liver Disease.* PLoS One, 2015. **10**(8): p. e0136822.PMC4556375. 10.1371/journal.pone.0136822.
20. Tang, X., M.M. Keenan, J. Wu, C.A. Lin, L. Dubois, J.W. Thompson, S.J. Freedland, S.K. Murphy, and J.T. Chi, *Comprehensive profiling of amino acid response uncovers unique methionine-deprived response dependent on intact creatine biosynthesis.* PLoS Genet, 2015. **11**(4): p. e1005158.PMC4388453. 10.1371/journal.pgen.1005158.
21. Maddineni, S., S. Nichenametla, R. Sinha, R.P. Wilson, and J.P. Richie, Jr., *Methionine restriction affects oxidative stress and glutathione-related redox pathways in the rat.* Exp Biol Med (Maywood), 2013. **238**(4): p. 392-910.1177/1535370213477988.

22. Miller, R.A., G. Buehner, Y. Chang, J.M. Harper, R. Sigler, and M. Smith-Wheelock, *Methionine-deficient diet extends mouse lifespan, slows immune and lens aging, alters glucose, T4, IGF-I and insulin levels, and increases hepatocyte MIF levels and stress resistance.* Aging Cell, 2005. **4**(3): p. 119-2510.1111/j.1474-9726.2005.00152.x.
23. Ables, G.P., A. Ouattara, T.G. Hampton, D. Cooke, F. Perodin, I. Augie, and D.S. Orentreich, *Dietary methionine restriction in mice elicits an adaptive cardiovascular response to hyperhomocysteinemia.* Sci Rep, 2015. **5**: p. 8886.PMC4351514. 10.1038/srep08886.
24. Huang, T.H., J.L. Lewis, H.S. Lin, L.T. Kuo, S.W. Mao, Y.S. Tai, M.S. Chang, G.P. Ables, C.E. Perrone, and R.S. Yang, *A methionine-restricted diet and endurance exercise decrease bone mass and extrinsic strength but increase intrinsic strength in growing male rats.* J Nutr, 2014. **144**(5): p. 621-3010.3945/jn.113.187922.
25. Pissios, P., S. Hong, A.R. Kennedy, D. Prasad, F.F. Liu, and E. Maratos-Flier, *Methionine and choline regulate the metabolic phenotype of a ketogenic diet.* Mol Metab, 2013. **2**(3): p. 306-13.PMC3773836. 10.1016/j.molmet.2013.07.003.
26. Hasek, B.E., L.K. Stewart, T.M. Henagan, A. Boudreau, N.R. Lenard, C. Black, J. Shin, P. Huypens, V.L. Malloy, E.P. Plaisance, R.A. Krajcik, N. Orentreich, and T.W. Gettys, *Dietary methionine restriction enhances metabolic flexibility and increases uncoupled respiration in both fed and fasted states.* Am J Physiol Regul Integr Comp Physiol, 2010. **299**(3): p. R728-39.PMC2944433. 10.1152/ajpregu.00837.2009.
27. Pakos-Zebrucka, K., I. Koryga, K. Mnich, M. Ljujic, A. Samali, and A.M. Gorman, *The integrated stress response.* EMBO Rep, 2016. **17**(10): p. 1374-1395.PMC5048378. 10.15252/embr.201642195.
28. Pettit, A.P., W.O. Jonsson, A.R. Bargoud, E.T. Mirek, F.F. Peelor, 3rd, Y. Wang, T.W. Gettys, S.R. Kimball, B.F. Miller, K.L. Hamilton, R.C. Wek, and T.G. Anthony, *Dietary Methionine Restriction Regulates Liver Protein Synthesis and Gene Expression Independently of Eukaryotic Initiation Factor 2 Phosphorylation in Mice.* J Nutr, 2017. **147**(6): p. 1031-1040.PMC5443467. 10.3945/jn.116.246710.
29. Anthony, T.G., B.J. McDaniel, R.L. Byerley, B.C. McGrath, D.R. Cavener, M.A. McNurlan, and R.C. Wek, *Preservation of liver protein synthesis during dietary leucine deprivation occurs at the expense of skeletal muscle mass in mice deleted for eIF2 kinase GCN2.* J Biol Chem, 2004. **279**(35): p. 36553-6110.1074/jbc.M404559200.
30. Guo, F. and D.R. Cavener, *The GCN2 eIF2alpha kinase regulates fatty-acid homeostasis in the liver during deprivation of an essential amino acid.* Cell Metab, 2007. **5**(2): p. 103-1410.1016/j.cmet.2007.01.001.
31. Maurin, A.C., C. Jousse, J. Averous, L. Parry, A. Bruhat, Y. Cherasse, H. Zeng, Y. Zhang, H.P. Harding, D. Ron, and P. Fafournoux, *The GCN2 kinase biases feeding behavior to maintain amino acid homeostasis in omnivores.* Cell Metab, 2005. **1**(4): p. 273-710.1016/j.cmet.2005.03.004.
32. Hao, S., J.W. Sharp, C.M. Ross-Inta, B.J. McDaniel, T.G. Anthony, R.C. Wek, D.R. Cavener, B.C. McGrath, J.B. Rudell, T.J. Koehnle, and D.W. Gietzen,

Uncharged tRNA and sensing of amino acid deficiency in mammalian piriform cortex. Science, 2005. **307**(5716): p. 1776-810.1126/science.1104882.

33. Leib, D.E. and Z.A. Knight, *Re-examination of Dietary Amino Acid Sensing Reveals a GCN2-Independent Mechanism.* Cell Rep, 2015. **13**(6): p. 1081-1089.PMC4836942. 10.1016/j.celrep.2015.09.055.
34. Zhang, P., B.C. McGrath, J. Reinert, D.S. Olsen, L. Lei, S. Gill, S.A. Wek, K.M. Vattem, R.C. Wek, S.R. Kimball, L.S. Jefferson, and D.R. Cavener, *The GCN2 eIF2alpha kinase is required for adaptation to amino acid deprivation in mice.* Mol Cell Biol, 2002. **22**(19): p. 6681-8.PMC134046.
35. Joshi, M.A., N.H. Jeoung, M. Obayashi, E.M. Hattab, E.G. Brocken, E.A. Liechty, M.J. Kubek, K.M. Vattem, R.C. Wek, and R.A. Harris, *Impaired growth and neurological abnormalities in branched-chain alpha-keto acid dehydrogenase kinase-deficient mice.* Biochem J, 2006. **400**(1): p. 153-62.PMC1635446. 10.1042/BJ20060869.
36. Novarino, G., P. El-Fishawy, H. Kayserili, N.A. Meguid, E.M. Scott, J. Schroth, J.L. Silhavy, M. Kara, R.O. Khalil, T. Ben-Omran, A.G. Ercan-Sencicek, A.F. Hashish, S.J. Sanders, A.R. Gupta, H.S. Hashem, D. Matern, S. Gabriel, L. Sweetman, Y. Rahimi, R.A. Harris, M.W. State, and J.G. Gleeson, *Mutations in BCKD-kinase lead to a potentially treatable form of autism with epilepsy.* Science, 2012. **338**(6105): p. 394-7.PMC3704165. 10.1126/science.1224631.
37. She, P., P. Bunpo, J.K. Cundiff, R.C. Wek, R.A. Harris, and T.G. Anthony, *General control nonderepressible 2 (GCN2) kinase protects oligodendrocytes and white matter during branched-chain amino acid deficiency in mice.* J Biol Chem, 2013. **288**(43): p. 31250-60.PMC3829435. 10.1074/jbc.M113.498469.
38. Ishimura, R., G. Nagy, I. Dotu, J.H. Chuang, and S.L. Ackerman, *Activation of GCN2 kinase by ribosome stalling links translation elongation with translation initiation.* Elife, 2016. **5**.PMC4917338. 10.7554/eLife.14295.
39. Chiu, I.M., E.T. Morimoto, H. Goodarzi, J.T. Liao, S. O'Keeffe, H.P. Phatnani, M. Muratet, M.C. Carroll, S. Levy, S. Tavazoie, R.M. Myers, and T. Maniatis, *A neurodegeneration-specific gene-expression signature of acutely isolated microglia from an amyotrophic lateral sclerosis mouse model.* Cell Rep, 2013. **4**(2): p. 385-401.PMC4272581. 10.1016/j.celrep.2013.06.018.
40. Orre, M., W. Kamphuis, L.M. Osborn, A.H.P. Jansen, L. Kooijman, K. Bossers, and E.M. Hol, *Isolation of glia from Alzheimer's mice reveals inflammation and dysfunction.* Neurobiol Aging, 2014. **35**(12): p. 2746-276010.1016/j.neurobiolaging.2014.06.004.
41. Qiu, H., J. Dong, C. Hu, C.S. Francklyn, and A.G. Hinnebusch, *The tRNA-binding moiety in GCN2 contains a dimerization domain that interacts with the kinase domain and is required for tRNA binding and kinase activation.* EMBO J, 2001. **20**(6): p. 1425-38.PMC145529. 10.1093/emboj/20.6.1425.
42. Wek, R.C., B.M. Jackson, and A.G. Hinnebusch, *Juxtaposition of domains homologous to protein kinases and histidyl-tRNA synthetases in GCN2 protein suggests a mechanism for coupling GCN4 expression to amino acid availability.* Proc Natl Acad Sci U S A, 1989. **86**(12): p. 4579-83.PMC287314.
43. Wek, R.C., M. Ramirez, B.M. Jackson, and A.G. Hinnebusch, *Identification of positive-acting domains in GCN2 protein kinase required for translational*

activation of GCN4 expression. Mol Cell Biol, 1990. **10**(6): p. 2820-31.PMC360643.

44. Wek, S.A., S. Zhu, and R.C. Wek, *The histidyl-tRNA synthetase-related sequence in the eIF-2 alpha protein kinase GCN2 interacts with tRNA and is required for activation in response to starvation for different amino acids.* Mol Cell Biol, 1995. **15**(8): p. 4497-506.PMC230689.
45. Zaborske, J.M., J. Narasimhan, L. Jiang, S.A. Wek, K.A. Dittmar, F. Freimoser, T. Pan, and R.C. Wek, *Genome-wide analysis of tRNA charging and activation of the eIF2 kinase Gcn2p.* J Biol Chem, 2009. **284**(37): p. 25254-67.PMC2757228. 10.1074/jbc.M109.000877.
46. Zaborske, J.M., X. Wu, R.C. Wek, and T. Pan, *Selective control of amino acid metabolism by the GCN2 eIF2 kinase pathway in Saccharomyces cerevisiae.* BMC Biochem, 2010. **11**: p. 29.PMC2921344. 10.1186/1471-2091-11-29.
47. Zhu, S., A.Y. Sobolev, and R.C. Wek, *Histidyl-tRNA synthetase-related sequences in GCN2 protein kinase regulate in vitro phosphorylation of eIF-2.* J Biol Chem, 1996. **271**(40): p. 24989-94
48. Wek, R.C., H.Y. Jiang, and T.G. Anthony, *Coping with stress: eIF2 kinases and translational control.* Biochem Soc Trans, 2006. **34**(Pt 1): p. 7-1110.1042/BST20060007.
49. De Sousa-Coelho, A.L., P.F. Marrero, and D. Haro, *Activating transcription factor 4-dependent induction of FGF21 during amino acid deprivation.* Biochem J, 2012. **443**(1): p. 165-7110.1042/BJ20111748.
50. Lees, E.K., E. Krol, L. Grant, K. Shearer, C. Wyse, E. Moncur, A.S. Bykowska, N. Mody, T.W. Gettys, and M. Delibegovic, *Methionine restriction restores a younger metabolic phenotype in adult mice with alterations in fibroblast growth factor 21.* Aging Cell, 2014. **13**(5): p. 817-27.PMC4331744. 10.1111/acel.12238.
51. Wanders, D., L.A. Forney, K.P. Stone, D.H. Burk, A. Pierse, and T.W. Gettys, *FGF21 Mediates the Thermogenic and Insulin-Sensitizing Effects of Dietary Methionine Restriction but Not Its Effects on Hepatic Lipid Metabolism.* Diabetes, 2017. **66**(4): p. 858-867.PMC5360300. 10.2337/db16-1212.
52. Al-Baghdadi, R.J.T., I.A. Nikonorova, E.T. Mirek, Y. Wang, J. Park, W.J. Belden, R.C. Wek, and T.G. Anthony, *Role of activating transcription factor 4 in the hepatic response to amino acid depletion by asparaginase.* Sci Rep, 2017. **7**(1): p. 1272.PMC5430736. 10.1038/s41598-017-01041-7.
53. Iwawaki, T., R. Akai, T. Toyoshima, N. Takeda, T.O. Ishikawa, and K.I. Yamamura, *Transgenic mouse model for imaging of ATF4 translational activation-related cellular stress responses in vivo.* Sci Rep, 2017. **7**: p. 46230.PMC5384252. 10.1038/srep46230.
54. Goetz, R., A. Beenken, O.A. Ibrahimi, J. Kalinina, S.K. Olsen, A.V. Eliseenkova, C. Xu, T.A. Neubert, F. Zhang, R.J. Linhardt, X. Yu, K.E. White, T. Inagaki, S.A. Kliewer, M. Yamamoto, H. Kurosu, Y. Ogawa, M. Kuro-o, B. Lanske, M.S. Razzaque, and M. Mohammadi, *Molecular insights into the klotho-dependent, endocrine mode of action of fibroblast growth factor 19 subfamily members.* Mol Cell Biol, 2007. **27**(9): p. 3417-28.PMC1899957. 10.1128/MCB.02249-06.
55. Goetz, R., M. Ohnishi, X. Ding, H. Kurosu, L. Wang, J. Akiyoshi, J. Ma, W. Gai, Y. Sidis, N. Pitteloud, O.M. Kuro, M.S. Razzaque, and M. Mohammadi, *Klotho*

coreceptors inhibit signaling by paracrine fibroblast growth factor 8 subfamily ligands. Mol Cell Biol, 2012. **32**(10): p. 1944-54.PMC3347405. 10.1128/MCB.06603-11.

56. Shimizu, N., T. Maruyama, N. Yoshikawa, R. Matsumiya, Y. Ma, N. Ito, Y. Tasaka, A. Kuribara-Souta, K. Miyata, Y. Oike, S. Berger, G. Schutz, S. Takeda, and H. Tanaka, *A muscle-liver-fat signalling axis is essential for central control of adaptive adipose remodelling.* Nat Commun, 2015. **6**: p. 6693.PMC4396397. 10.1038/ncomms7693.
57. Asada, R., S. Kanemoto, K. Matsuhisa, K. Hino, M. Cui, X. Cui, M. Kaneko, and K. Imaizumi, *IRE1alpha-XBP1 is a novel branch in the transcriptional regulation of Ucp1 in brown adipocytes.* Sci Rep, 2015. **5**: p. 16580.PMC4644985. 10.1038/srep16580.
58. Wan, X.S., X.H. Lu, Y.C. Xiao, Y. Lin, H. Zhu, T. Ding, Y. Yang, Y. Huang, Y. Zhang, Y.L. Liu, Z.M. Xu, J. Xiao, and X.K. Li, *ATF4- and CHOP-dependent induction of FGF21 through endoplasmic reticulum stress.* Biomed Res Int, 2014. **2014**: p. 807874.PMC4037570. 10.1155/2014/807874.
59. Uebanso, T., Y. Taketani, H. Yamamoto, K. Amo, H. Ominami, H. Arai, Y. Takei, M. Masuda, A. Tanimura, N. Harada, H. Yamanaka-Okumura, and E. Takeda, *Paradoxical regulation of human FGF21 by both fasting and feeding signals: is FGF21 a nutritional adaptation factor?* PLoS One, 2011. **6**(8): p. e22976.PMC3148241. 10.1371/journal.pone.0022976.
60. Bielohuby, M., D. Menhofer, H. Kirchner, B.J. Stoehr, T.D. Muller, P. Stock, M. Hempel, K. Stemmer, P.T. Pfluger, E. Kienzle, B. Christ, M.H. Tschop, and M. Bidlingmaier, *Induction of ketosis in rats fed low-carbohydrate, high-fat diets depends on the relative abundance of dietary fat and protein.* Am J Physiol Endocrinol Metab, 2011. **300**(1): p. E65-7610.1152/ajpendo.00478.2010.
61. Potthoff, M.J., T. Inagaki, S. Satapati, X. Ding, T. He, R. Goetz, M. Mohammadi, B.N. Finck, D.J. Mangelsdorf, S.A. Kliewer, and S.C. Burgess, *FGF21 induces PGC-1alpha and regulates carbohydrate and fatty acid metabolism during the adaptive starvation response.* Proc Natl Acad Sci U S A, 2009. **106**(26): p. 10853-8.PMC2705613. 10.1073/pnas.0904187106.
62. Solon-Biet, S.M., V.C. Cogger, T. Pulpitel, M. Heblinski, D. Wahl, A.C. McMahon, A. Warren, J. Durrant-Whyte, K.A. Walters, J.R. Krycer, F. Ponton, R. Gokarn, J.A. Wali, K. Ruohonen, A.D. Conigrave, D.E. James, D. Raubenheimer, C.D. Morrison, D.G. Le Couteur, and S.J. Simpson, *Defining the Nutritional and Metabolic Context of FGF21 Using the Geometric Framework.* Cell Metab, 2016. **24**(4): p. 555-56510.1016/j.cmet.2016.09.001.
63. Laeger, T., T.M. Henagan, D.C. Albarado, L.M. Redman, G.A. Bray, R.C. Noland, H. Munzberg, S.M. Hutson, T.W. Gettys, M.W. Schwartz, and C.D. Morrison, *FGF21 is an endocrine signal of protein restriction.* J Clin Invest, 2014. **124**(9): p. 3913-22.PMC4153701. 10.1172/JCI74915.
64. Salminen, A., K. Kaarniranta, and A. Kauppinen, *Regulation of longevity by FGF21: Interaction between energy metabolism and stress responses.* Ageing Res Rev, 2017. **37**: p. 79-9310.1016/j.arr.2017.05.004.

65. Salminen, A., K. Kaarniranta, and A. Kauppinen, *Integrated stress response stimulates FGF21 expression: Systemic enhancer of longevity.* Cell Signal, 2017. **40**: p. 10-2110.1016/j.cellsig.2017.08.009.
66. Kim, K.H. and M.S. Lee, *FGF21 as a mediator of adaptive responses to stress and metabolic benefits of anti-diabetic drugs.* J Endocrinol, 2015. **226**(1): p. R1-1610.1530/JOE-15-0160.
67. Liu, J., Y. Xu, Y. Hu, and G. Wang, *The role of fibroblast growth factor 21 in the pathogenesis of non-alcoholic fatty liver disease and implications for therapy.* Metabolism, 2015. **64**(3): p. 380-9010.1016/j.metabol.2014.11.009.
68. Coskun, T., H.A. Bina, M.A. Schneider, J.D. Dunbar, C.C. Hu, Y. Chen, D.E. Moller, and A. Kharitonenkov, *Fibroblast growth factor 21 corrects obesity in mice.* Endocrinology, 2008. **149**(12): p. 6018-2710.1210/en.2008-0816.
69. Xu, J., D.J. Lloyd, C. Hale, S. Stanislaus, M. Chen, G. Sivits, S. Vonderfecht, R. Hecht, Y.S. Li, R.A. Lindberg, J.L. Chen, D.Y. Jung, Z. Zhang, H.J. Ko, J.K. Kim, and M.M. Veniant, *Fibroblast growth factor 21 reverses hepatic steatosis, increases energy expenditure, and improves insulin sensitivity in diet-induced obese mice.* Diabetes, 2009. **58**(1): p. 250-9.PMC2606881. 10.2337/db08-0392.
70. Xu, P., Y. Zhang, Y. Liu, Q. Yuan, L. Song, M. Liu, Z. Liu, Y. Yang, J. Li, D. Li, and G. Ren, *Fibroblast growth factor 21 attenuates hepatic fibrogenesis through TGF-beta/smad2/3 and NF-kappaB signaling pathways.* Toxicol Appl Pharmacol, 2016. **290**: p. 43-5310.1016/j.taap.2015.11.012.
71. Wanders, D., K.P. Stone, L.A. Forney, C.C. Cortez, K.N. Dille, J. Simon, M. Xu, E.C. Hotard, I.A. Nikonorova, A.P. Pettit, T.G. Anthony, and T.W. Gettys, *Role of GCN2-Independent Signaling Through a Noncanonical PERK/NRF2 Pathway in the Physiological Responses to Dietary Methionine Restriction.* Diabetes, 2016. **65**(6): p. 1499-510.PMC4878423. 10.2337/db15-1324.
72. Mazor, K.M. and M.H. Stipanuk, *GCN2- and eIF2alpha-phosphorylation-independent, but ATF4-dependent, induction of CARE-containing genes in methionine-deficient cells.* Amino Acids, 2016. **48**(12): p. 2831-2842.PMC5107328. 10.1007/s00726-016-2318-9.
73. Wang, C., Z. Huang, Y. Du, Y. Cheng, S. Chen, and F. Guo, *ATF4 regulates lipid metabolism and thermogenesis.* Cell Res, 2010. **20**(2): p. 174-8410.1038/cr.2010.4.
74. Wang, C., T. Xia, Y. Du, Q. Meng, H. Li, B. Liu, S. Chen, and F. Guo, *Effects of ATF4 on PGC1alpha expression in brown adipose tissue and metabolic responses to cold stress.* Metabolism, 2013. **62**(2): p. 282-910.1016/j.metabol.2012.07.017.
75. Deng, J., F. Yuan, Y. Guo, Y. Xiao, Y. Niu, Y. Deng, X. Han, Y. Guan, S. Chen, and F. Guo, *Deletion of ATF4 in AgRP Neurons Promotes Fat Loss Mainly via Increasing Energy Expenditure.* Diabetes, 2017. **66**(3): p. 640-65010.2337/db16-0954.
76. Xiao, Y., Y. Deng, F. Yuan, T. Xia, H. Liu, Z. Li, Z. Liu, H. Ying, Y. Liu, Q. Zhai, S. Chen, and F. Guo, *ATF4/ATG5 Signaling in Hypothalamic Proopiomelanocortin Neurons Regulates Fat Mass via Affecting Energy Expenditure.* Diabetes, 2017. **66**(5): p. 1146-115810.2337/db16-1546.
77. De Sousa-Coelho, A.L., J. Relat, E. Hondares, A. Perez-Marti, F. Ribas, F. Villarroya, P.F. Marrero, and D. Haro, *FGF21 mediates the lipid metabolism*

response to amino acid starvation. J Lipid Res, 2013. **54**(7): p. 1786-97.PMC3679382. 10.1194/jlr.M033415.

78. Song, P., C. Zechner, G. Hernandez, J. Canovas, Y. Xie, V. Sondhi, M. Wagner, V. Stadlbauer, A. Horvath, B. Leber, M.C. Hu, O.W. Moe, D.J. Mangelsdorf, and S.A. Kliewer, *The Hormone FGF21 Stimulates Water Drinking in Response to Ketogenic Diet and Alcohol.* Cell Metab, 2018. **27**(6): p. 1338-1347 e4.PMC5990458. 10.1016/j.cmet.2018.04.001.
79. Sears, T.K. and J.M. Angelastro, *The transcription factor ATF5: role in cellular differentiation, stress responses, and cancer.* Oncotarget, 2017. **8**(48): p. 84595-84609.PMC5663623. 10.18632/oncotarget.21102.
80. Mallo, G.V., F. Fiedler, E.L. Calvo, E.M. Ortiz, S. Vasseur, V. Keim, J. Morisset, and J.L. Iovanna, *Cloning and expression of the rat p8 cDNA, a new gene activated in pancreas during the acute phase of pancreatitis, pancreatic development, and regeneration, and which promotes cellular growth.* J Biol Chem, 1997. **272**(51): p. 32360-9
81. Goruppi, S. and J.L. Iovanna, *Stress-inducible protein p8 is involved in several physiological and pathological processes.* J Biol Chem, 2010. **285**(3): p. 1577-81.PMC2804314. 10.1074/jbc.R109.080887.
82. Kong, D.K., S.P. Georgescu, C. Cano, M.J. Aronovitz, J.L. Iovanna, R.D. Patten, J.M. Kyriakis, and S. Goruppi, *Deficiency of the transcriptional regulator p8 results in increased autophagy and apoptosis, and causes impaired heart function.* Mol Biol Cell, 2010. **21**(8): p. 1335-49.PMC2854092. 10.1091/mbc.E09-09-0818.
83. Vasseur, S., A. Hoffmeister, A. Garcia-Montero, M. Barthet, L. Saint-Michel, P. Berthezene, F. Fiedler, D. Closa, J.C. Dagorn, and J.L. Iovanna, *Mice with targeted disruption of p8 gene show increased sensitivity to lipopolysaccharide and DNA microarray analysis of livers reveals an aberrant gene expression response.* BMC Gastroenterol, 2003. **3**: p. 25.PMC212298. 10.1186/1471-230X-3-25.
84. Gironella, M., C. Malicet, C. Cano, M.J. Sandi, T. Hamidi, R.M. Tauil, M. Baston, P. Valaco, S. Moreno, F. Lopez, J.L. Neira, J.C. Dagorn, and J.L. Iovanna, *p8/nupr1 regulates DNA-repair activity after double-strand gamma irradiation-induced DNA damage.* J Cell Physiol, 2009. **221**(3): p. 594-60210.1002/jcp.21889.
85. Taieb, D., C. Malicet, S. Garcia, P. Rocchi, C. Arnaud, J.C. Dagorn, J.L. Iovanna, and S. Vasseur, *Inactivation of stress protein p8 increases murine carbon tetrachloride hepatotoxicity via preserved CYP2E1 activity.* Hepatology, 2005. **42**(1): p. 176-8210.1002/hep.20759.
86. Tang, B., Q. Li, X.H. Zhao, H.G. Wang, N. Li, Y. Fang, K. Wang, Y.P. Jia, P. Zhu, J. Gu, J.X. Li, Y.J. Jiao, W.D. Tong, M. Wang, Q.M. Zou, F.C. Zhu, and X.H. Mao, *Shiga toxins induce autophagic cell death in intestinal epithelial cells via the endoplasmic reticulum stress pathway.* Autophagy, 2015. **11**(2): p. 344-54.PMC4502731. 10.1080/15548627.2015.1023682.
87. Averous, J., S. Lambert-Langlais, Y. Cherasse, V. Carraro, L. Parry, W. B'Chir, C. Jousse, A.C. Maurin, A. Bruhat, and P. Fafournoux, *Amino acid deprivation*

regulates the stress-inducible gene p8 via the GCN2/ATF4 pathway. Biochem Biophys Res Commun, 2011. **413**(1): p. 24-910.1016/j.bbrc.2011.08.028.

88. Maida, A., A. Zota, K.A. Sjoberg, J. Schumacher, T.P. Sijmonsma, A. Pfenninger, M.M. Christensen, T. Gantert, J. Fuhrmeister, U. Rothermel, D. Schmoll, M. Heikenwalder, J.L. Iovanna, K. Stemmer, B. Kiens, S. Herzig, and A.J. Rose, *A liver stress-endocrine nexus promotes metabolic integrity during dietary protein dilution.* J Clin Invest, 2016. **126**(9): p. 3263-78.PMC5004939. 10.1172/JCI85946.
89. Vasseur, S., G.V. Mallo, A. Garcia-Montero, E.M. Ortiz, F. Fiedler, E. Canepa, S. Moreno, and J.L. Iovanna, *Structural and functional characterization of the mouse p8 gene: promotion of transcription by the CAAT-enhancer binding protein alpha (C/EBPalpha) and C/EBPbeta trans-acting factors involves a C/EBP cis-acting element and other regions of the promoter.* Biochem J, 1999. **343 Pt 2**: p. 377-83.PMC1220564.
90. Jin, H.O., S.K. Seo, S.H. Woo, T.B. Choe, S.I. Hong, J.I. Kim, and I.C. Park, *Nuclear protein 1 induced by ATF4 in response to various stressors acts as a positive regulator on the transcriptional activation of ATF4.* IUBMB Life, 2009. **61**(12): p. 1153-810.1002/iub.271.
91. Gomez-Samano, M.A., M. Grajales-Gomez, J.M. Zuarth-Vazquez, M.F. Navarro-Flores, M. Martinez-Saavedra, O.A. Juarez-Leon, M.G. Morales-Garcia, V.M. Enriquez-Estrada, F.J. Gomez-Perez, and D. Cuevas-Ramos, *Fibroblast growth factor 21 and its novel association with oxidative stress.* Redox Biol, 2017. **11**: p. 335-341.PMC5200873. 10.1016/j.redox.2016.12.024.
92. He, C.H., P. Gong, B. Hu, D. Stewart, M.E. Choi, A.M. Choi, and J. Alam, *Identification of activating transcription factor 4 (ATF4) as an Nrf2-interacting protein. Implication for heme oxygenase-1 gene regulation.* J Biol Chem, 2001. **276**(24): p. 20858-6510.1074/jbc.M101198200.
93. Furusawa, Y., A. Uruno, Y. Yagishita, C. Higashi, and M. Yamamoto, *Nrf2 induces fibroblast growth factor 21 in diabetic mice.* Genes Cells, 2014. **19**(12): p. 864-7810.1111/gtc.12186.
94. Christodoulides, C., P. Dyson, D. Sprecher, K. Tsintzas, and F. Karpe, *Circulating fibroblast growth factor 21 is induced by peroxisome proliferator-activated receptor agonists but not ketosis in man.* J Clin Endocrinol Metab, 2009. **94**(9): p. 3594-60110.1210/jc.2009-0111.
95. Lundasen, T., M.C. Hunt, L.M. Nilsson, S. Sanyal, B. Angelin, S.E. Alexson, and M. Rudling, *PPARalpha is a key regulator of hepatic FGF21.* Biochem Biophys Res Commun, 2007. **360**(2): p. 437-4010.1016/j.bbrc.2007.06.068.
96. Carracedo, A., A. Egia, M. Guzman, and G. Velasco, *p8 Upregulation sensitizes astrocytes to oxidative stress.* FEBS Lett, 2006. **580**(6): p. 1571-510.1016/j.febslet.2006.01.084.
97. Jiang, S., C. Yan, Q.C. Fang, M.L. Shao, Y.L. Zhang, Y. Liu, Y.P. Deng, B. Shan, J.Q. Liu, H.T. Li, L. Yang, J. Zhou, Z. Dai, Y. Liu, and W.P. Jia, *Fibroblast growth factor 21 is regulated by the IRE1alpha-XBP1 branch of the unfolded protein response and counteracts endoplasmic reticulum stress-induced hepatic steatosis.* J Biol Chem, 2014. **289**(43): p. 29751-65.PMC4207989. 10.1074/jbc.M114.565960.

98. Koyanagi, S., A.M. Hamdan, M. Horiguchi, N. Kusunose, A. Okamoto, N. Matsunaga, and S. Ohdo, *cAMP-response element (CRE)-mediated transcription by activating transcription factor-4 (ATF4) is essential for circadian expression of the Period2 gene.* J Biol Chem, 2011. **286**(37): p. 32416-23.PMC3173173. 10.1074/jbc.M111.258970.
99. Yu, H., F. Xia, K.S. Lam, Y. Wang, Y. Bao, J. Zhang, Y. Gu, P. Zhou, J. Lu, W. Jia, and A. Xu, *Circadian rhythm of circulating fibroblast growth factor 21 is related to diurnal changes in fatty acids in humans.* Clin Chem, 2011. **57**(5): p. 691-70010.1373/clinchem.2010.155184.